

LA-UR-

12-00015

Approved for public release;
distribution is unlimited.

Title: Frictional Interactions at Sliding Metal Interfaces

Author(s): James E Hammerberg, XCP-5
Ramon J Ravelo, XCP-5
Timothy C Germann, T-1
Brad L Holian, T-1

Intended for: Int. Symposium on Plasticity and Its Current Applications
San Juan, Puerto Rico, Jan. 5-8, 2012



Los Alamos National Laboratory, an affirmative action/equal opportunity employer, is operated by the Los Alamos National Security, LLC for the National Nuclear Security Administration of the U.S. Department of Energy under contract DE-AC52-06NA25396. By acceptance of this article, the publisher recognizes that the U.S. Government retains a nonexclusive, royalty-free license to publish or reproduce the published form of this contribution, or to allow others to do so, for U.S. Government purposes. Los Alamos National Laboratory requests that the publisher identify this article as work performed under the auspices of the U.S. Department of Energy. Los Alamos National Laboratory strongly supports academic freedom and a researcher's right to publish; as an institution, however, the Laboratory does not endorse the viewpoint of a publication or guarantee its technical correctness.

Frictional Interactions at Sliding Metal Interfaces

James E. Hammerberg, R. Ravelo, T.C. Germann, J. Milhans and B.L. Holian
Los Alamos National Laboratory
Los Alamos, NM

Plasticity2012
San Juan, Puerto Rico
Jan. 3-8, 2012

Overview

- Experimental background for metal/metal sliding
- Large-scale Non-Equilibrium Molecular Dynamics (NEMD) simulations to characterize physical mechanisms
- Generic properties of the velocity dependence of the frictional Force
- Large systems and scaling
- Defective and polycrystalline samples
- Summary

Experimental Overview – Velocity Dependence

High-speed levitated sphere experiments of Bowden and collaborators demonstrated significant weakening of the frictional force with increasing velocities to 700 m/s.

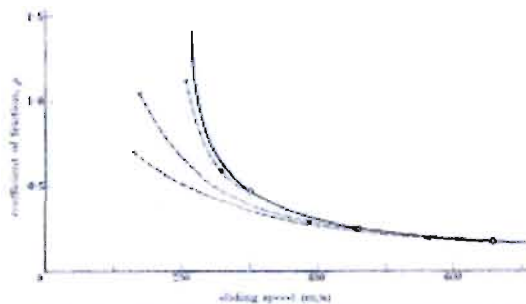
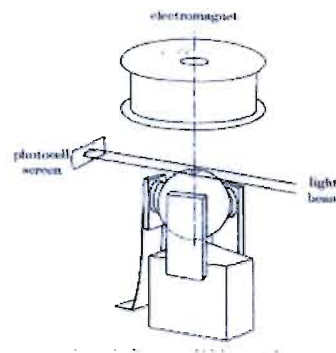


FIGURE 5. The friction of steel on copper. Load 30g. The dashed curves are for the deceleration of balls of 1 cm diameter from different initial sliding speeds.

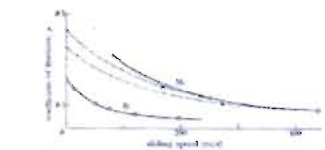


FIGURE 6. The friction of steel on itself and on iron. Loads 10g and 20g respectively.

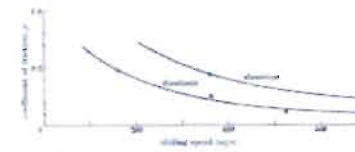


FIGURE 7. The friction of steel on aluminium and aluminium. Load 20g.

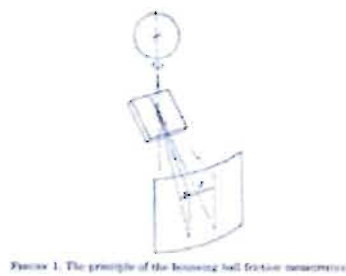


FIGURE 1. The principle of the falling ball friction measurement.

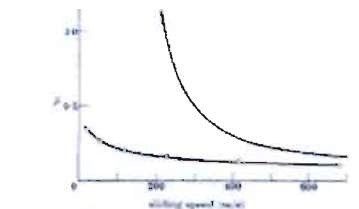


FIGURE 17. Steel sliding on copper. Comparison of μ from bearing ball experiments (○) with μ from light load experiments (—).

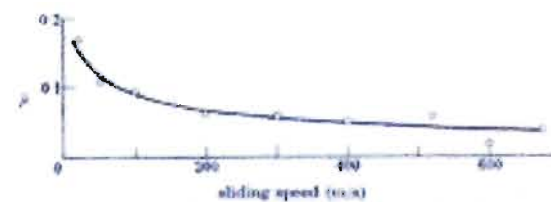


FIGURE 18. Steel sliding on itself. β as a function of sliding speed.

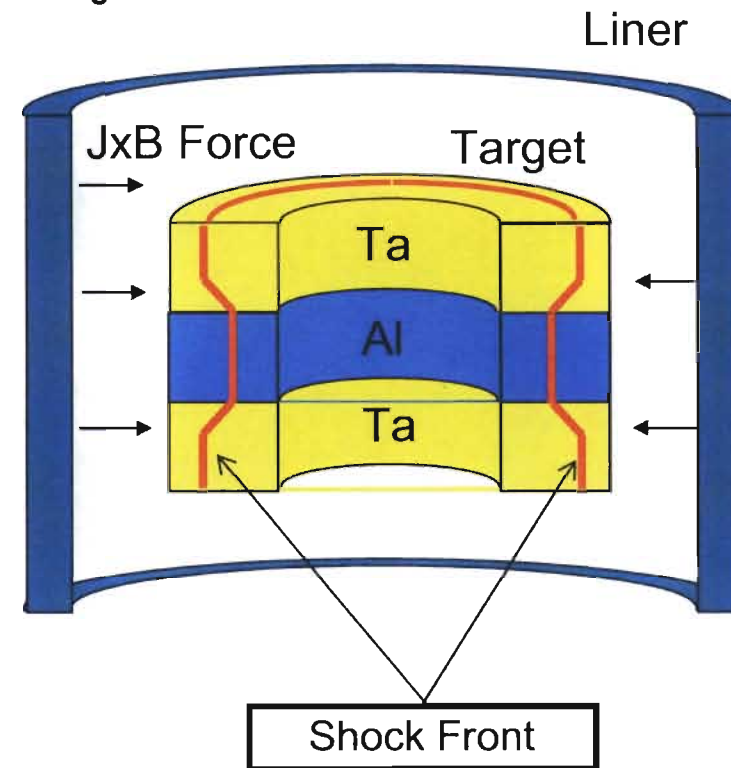
Bowden, F.P. and Freitag, E.H., 1958, "The Friction of Solids at Very High Speeds", Proc. Roy. Soc. (Lond.) Ser. A, Vol. 248, pp. 350-367.

Bowden, F.P. and Persson, P.A., 1961, "Deformation, Heating and Melting of Solids in High-Speed Friction", Proc. Roy. Soc. (Lond.) Ser. A, Vol. 260 pp. 433-458.

Experimental Overview – Velocity Dependence

Atlas pulsed power experiments measured similar velocity weakening at a Ta/Al interface at 15 GPa for sliding velocities between 360 and 700 m/s.

- Hollow, cylindrical “lifesaver” sandwich target enabled diagnostic access and reduced end effects
- Low Cs material (Ta)
- High Cs material (Al)
- Low Cs material (Ta)
- 2-interfaces/experiment (2/6/ μ m RMS finish)
- Thick liner (7 mm initial, 10 mm at impact)
- Maintained shocked state longer
- Produced greater interface displacement
- Must be transparent to radiography
- 1.5-2.5 km/s impact velocity



Experimental Overview – Velocity Dependence

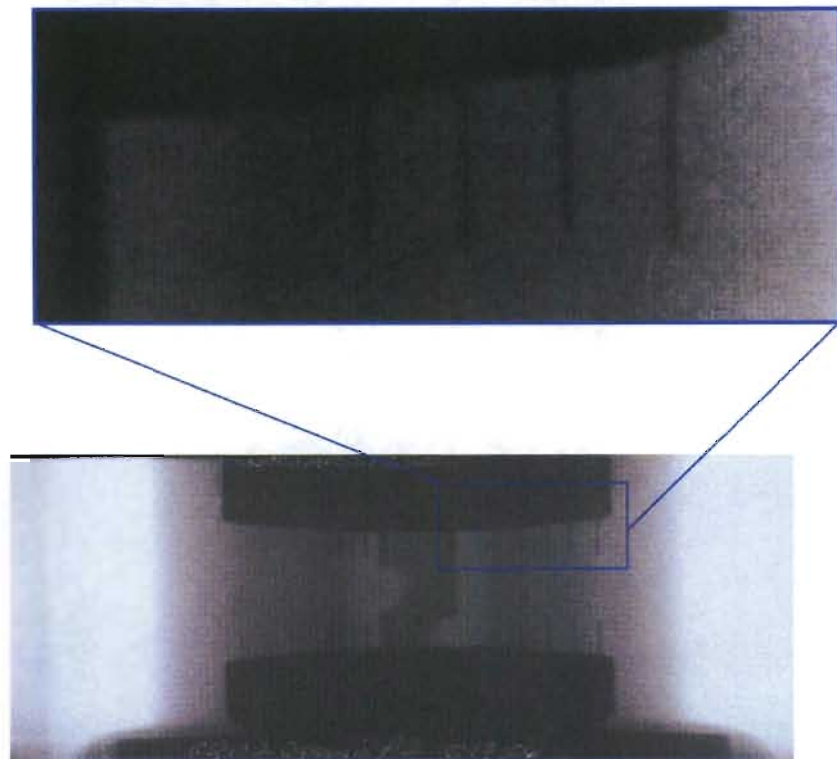
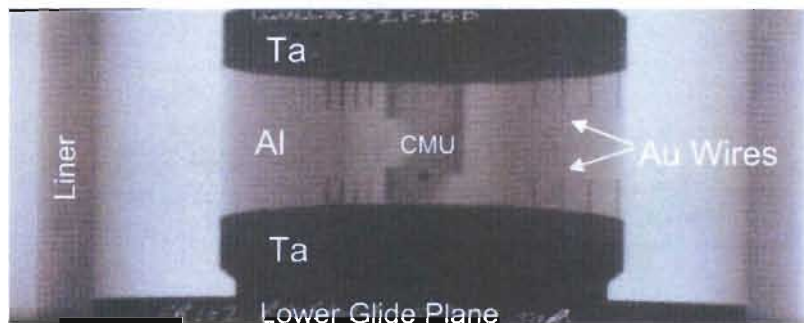
Atlas pulsed power facility at NTS provided reproducible, tunable drive.



- 26 MJ stored energy, 6 ms rise time
- Symmetric, cylindrically
- 1/3, 2/3, 3/3 bank configurations (and others)

Experimental Overview – Velocity Dependence

Transverse radiography
measured bending of 0.4 mm
Au wires. Lagrangian analysis
determines F/A.



Dynamic Radiograph ($t = 22.2 \mu\text{s}$)

Experimental Overview – Velocity Dependence

Lagrangian analysis showed velocity weakening.

Expt.	V_{impact} (mm/ μs)	P (GPa)	Δt (μs)	F_{tang}/A (GPa)	Yield Strength (GPa)	$\langle V_{\text{int}} \rangle$ (mm/ μs)
FR102	1.3	13	3.58	0.60	0.8	0.36
FR103	1.5	15	3.727	0.09	0.9	0.56
FR101	1.7	18	2.408	< 0.09	1.0	0.70

Experimental Overview – Velocity Dependence

- Explosively driven experiments



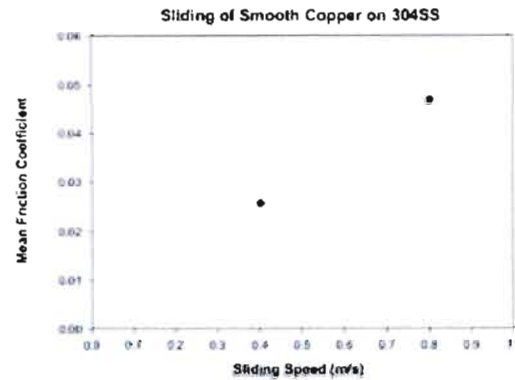
Figure 2. The F80 experiment. The stainless steel and stainless steel (inner) components were machined to a surface roughness of $\leq 2 \mu\text{m}$ and were flat such that the maximum gap that could exist between the sliding surfaces was $\leq 2 \mu\text{m}$. The components were held in contact by gravity.



Figure 5. The steel component recovered from F80-3. The outlines of the surface markings mirror the corresponding outlines on the aluminum block (see figure 6).

[R.E. Winter et al., 2006, "Mechanisms of Shock-Induced Dynamic Friction," *J. Phys. D*, Vol. 39, pp. 5043-5053]

- Rotating Barrel Gas Gun



Experimental Overview – Velocity Dependence

- Plate-impact pressure-shear friction experiment

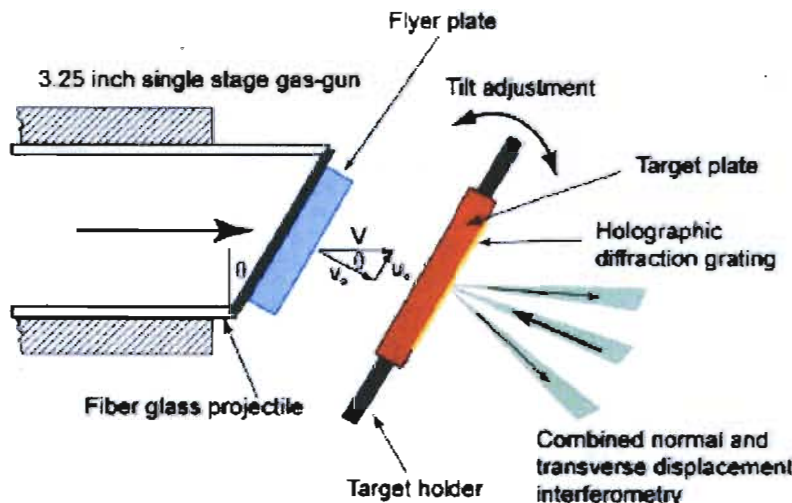
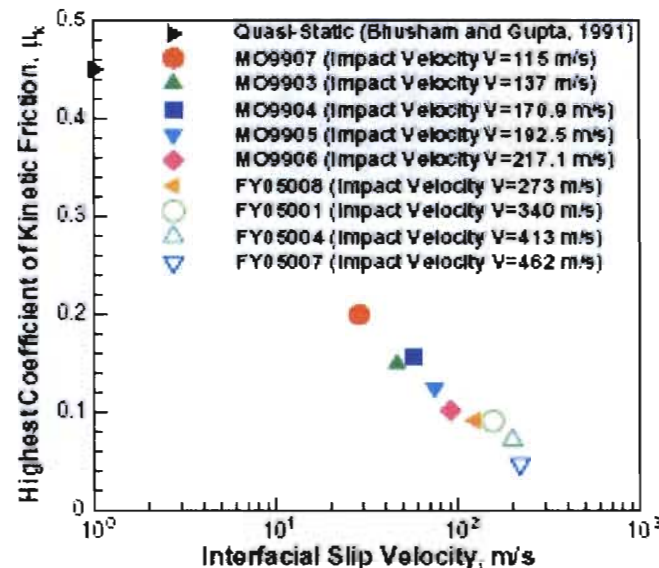


Fig. 1. Schematic of the plate-impact pressure-shear friction experiment.



[F. Yuan, N.-S. Liou and V. Prakash, 2009, "High-Speed Frictional Slip at Metal-on-Metal Interfaces," Int. J. Plast., Vol. 25, pp. 612-634.]

Experimental Overview – Structural Transformation

- Dry sliding induces subgrain nanostructure and highly strained graded microstructure in ductile metals.

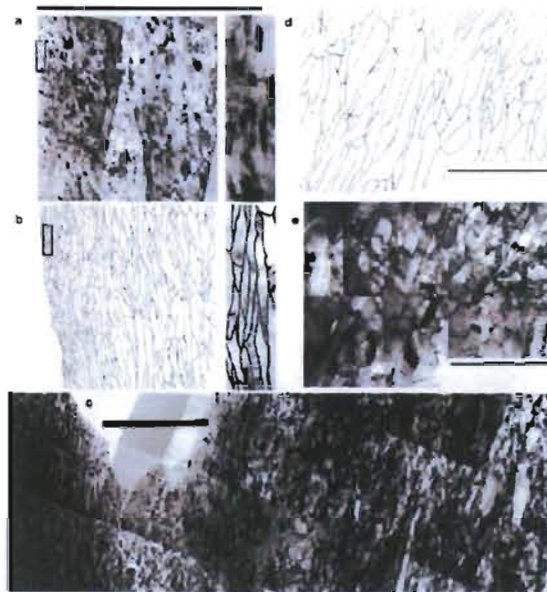


FIG. 1: Graded nanostructures produced by friction deformation as viewed in cross section by TEM. (a) Micrograph and (b) tracing of extended boundaries in Cu following sliding under 12 MPa applied normal pressure; the left side is coincident with the surface. Rectangular boxes show location of the adjacent high magnification regions illustrating a layer with 12 nm average boundary spacing. These rectangles are 70 nm wide. (c) Following sliding with 22.5 MPa pressure; the surface is coincident with the left side. (d) The pair grain regions underneath the scale marker in the hole produced when using the 1224 ball. (d) Tracing and micrograph of a sample in (c) but at 20 nm below the surface. Scale markers are 2 nm.

[D.A. Hughes and N. Hansen, 2001, "Graded Nanostructures Induced by Sliding and Exhibiting Universal Behavior," Phys. Rev. Lett. Vol. 87, pp. 1355031-1355034.]

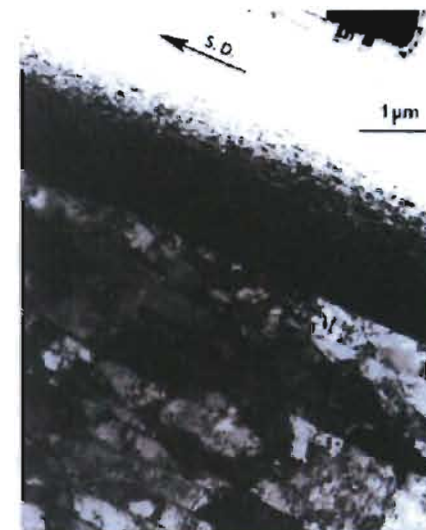


Figure 1: TEM micrograph for OFHC Cu sliding on 440C stainless steel, sliding at 1 cm/sec for 12 m at normal load 66.6. Longitudinal section. Arrow denotes sliding direction. From Ref. (22).

[D.A. Rigney, 1988, "Sliding Wear of Metals," Ann. Rev. Mater. Sci., Vol. 18, pp.141-163.]

Experimental Overview – Structural Transformation

- Cu pin on disk and Al explosively driven experiments show nanocrystalline regions and highly strained regions at the sliding interface.

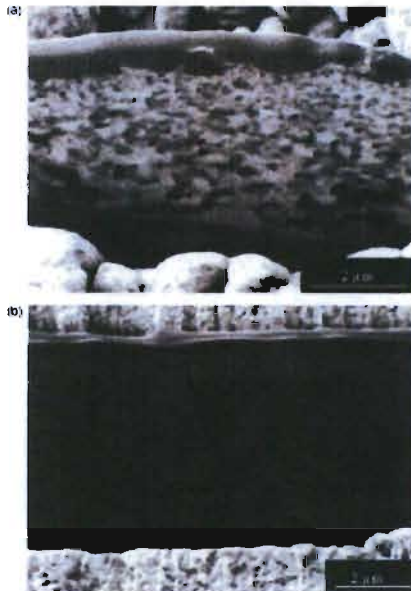


Fig. 4. FIB ion channeling images of transverse cross-sections from the disk wear track showing (a) a gradient of increasing grain size below the wear track for a 0.25 m/s test and (b) the abrupt transition from a subsurface nanocrystalline region to a large grained region for a 1.5 m/s test.

[Andrew Emge, S. Karthikeyan, H.J. Kim and D.A. Rigney, 2007, "The Effect of Sliding Velocity on the Tribological Behavior of Copper," Wear, Vol. 263, pp. 614-618]



Fig. 5. TEM micrograph of a cross-section of tested AWS53 aluminum. A thin nanocrystalline layer (left side) and adjacent heavily deformed material are shown. The resolution of the structure is higher here than in Fig. 7. Using both types of images provides the desired resolution and demonstrates that the structures are not simply local effects.

[H.J. Kim, A. Emge, R.E. Winter, P.T. Keightley, W.J. Kim, M.L. Falk and D.A. Rigney, 2009, "Nanostructures Generated by Explosively Driven Friction: Experiments and Molecular Dynamics Simulations," *Acta Mater.* Doi:10.1016/j.actamat.2009.07.034]

Experimental Overview – Material Mixing

- Nanocrystalline mixing layer (A) at a Cu/SS interface

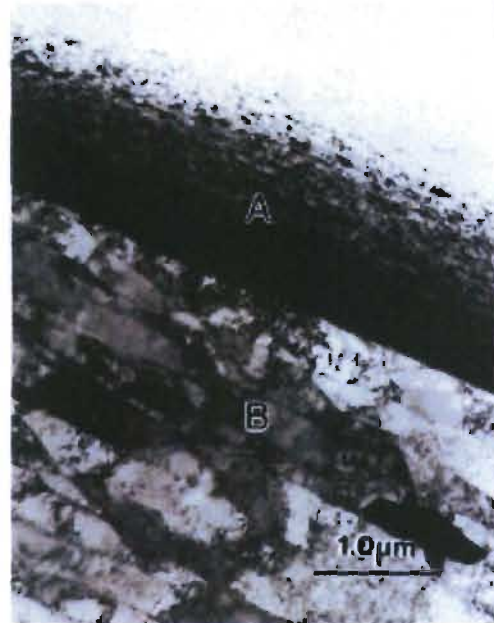


Fig. 3. TEM image of longitudinal section of OFHC copper block after sliding against 440C steel ring. Note sharp demarcation between nanocrystalline mixed material and deformation substructure (subgrains of base material. Same sample and conditions as in Fig. 1.

[D.A. Rigney, 2000, "Transfer, Mixing and Associated Chemical and Mechanical Processes during the Sliding of Ductile Metals," Wear, Vol. 245, pp. 1-9]

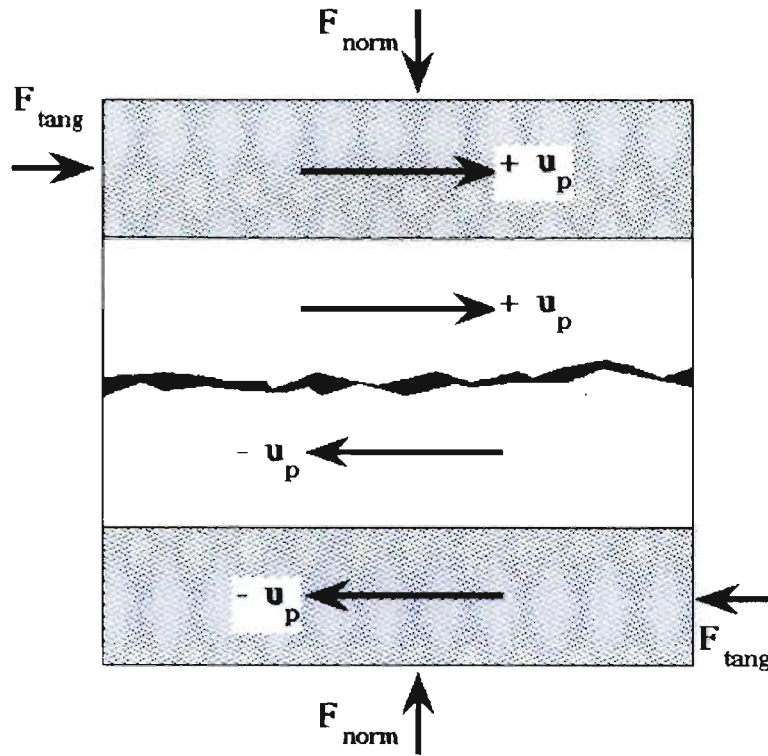
Summary – Experimental

- Frictional force at metal-metal interfaces exhibits a decrease with increasing sliding velocity at high velocities (velocity weakening).
- The near-surface microstructure transforms to smaller length scale structure that is graded and exhibits very high plastic strains in regions of tens of microns from the sliding interface.
- There is evidence for a mechanically mixed layer of nanoscale material at the sliding interface.

Large-Scale NEMD Simulations of the Tangential Force as a Function of Sliding Velocity and Compression

- Experimental data for the tangential force as a function of velocity and compression are sparse and difficult to obtain dynamically.
- Integral experiments have been carried out by R. Winter, et al., using high-explosive drive. Pulsed power radiographic experiments have also been carried out (G. Kyrala, R. Faehl, C. Rousculp, et al., LANL – Pegasus, Atlas experiments), which are more nearly direct measurements of the tangential force.
- Rotating-Barrel gas gun experiments (P. Rightley, P. Crawford and K. Rainey, LANL) allow measurements of F_t at velocities less than 100 m/s.
- Pressure-shear measurements have been carried out to 450 m/s (v. Prakash et al.).
- Large-scale Non-Equilibrium Molecular Dynamics (NEMD) allows for microscopic interrogation of physical mechanisms at relevant sliding rates (0–1 km/s).

NEMD Simulations



Typical system sizes: 10^6 atoms

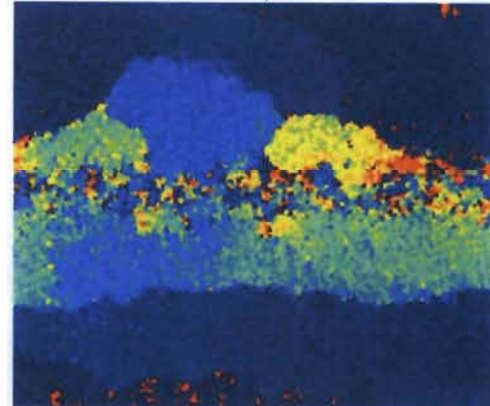
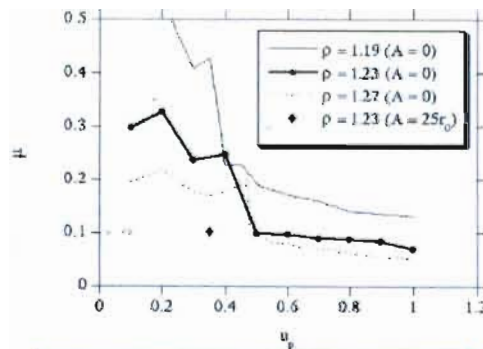
Typical integration times: 1 ns

[J.E. Hammerberg, B.L. Holian, J. Roeder, A.R. Bishop and S.J. Zhou, 1998, "Nonlinear Dynamics and the Problem of Slip at Material Interfaces," *Physica D*, Vol. 123, pp. 330-340.
J.E. Hammerberg and B.L. Holian, 2004, "Simulation Methods for Interfacial Friction in Solids," in *Surface Modification and Mechanisms*, G.E. Totten and H. Liang, eds., pp. 723-749.]

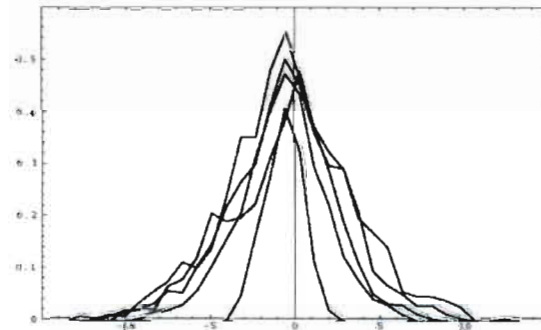
Slide 15

NEMD Simulations

- Initial Cu/Cu two-dimensional simulations showed all three experimental features: velocity weakening, structural transformation and mechanical mixing.



Cu(2D) $P=30\text{GPa}$, $v = 0.12c_t$, Mechanical Mixing



Times: 100, 200, 300, 400, 500 t_0

Material Pairs Investigated with NEMD

Material Pairs Investigated

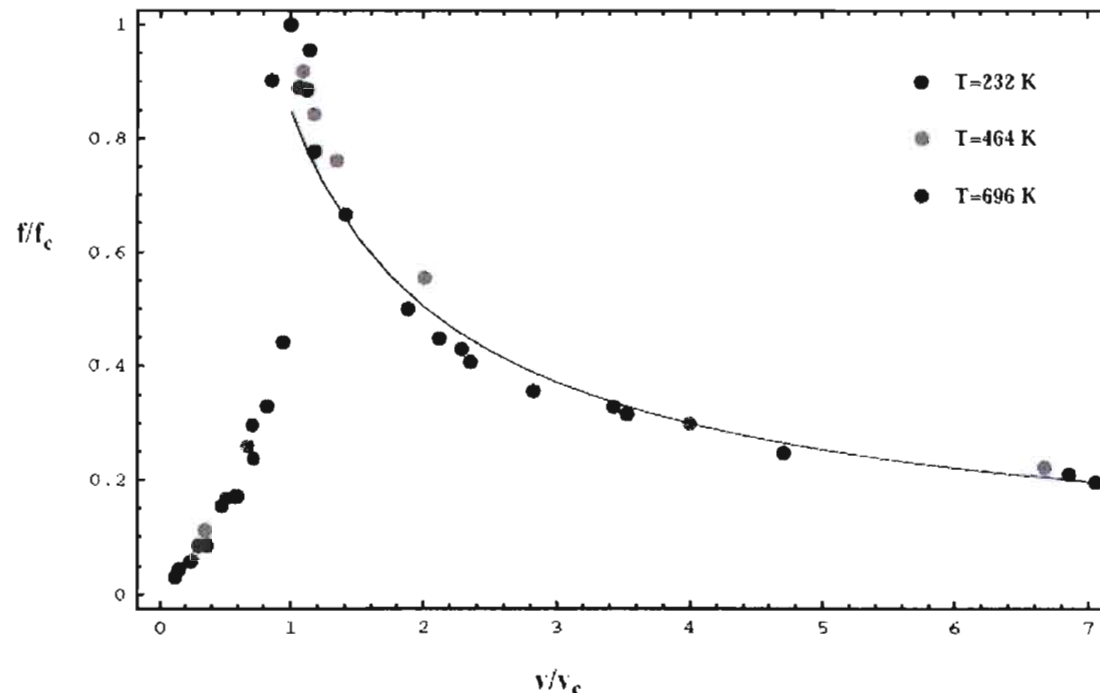
Tribo-Pair	Dimension	Vmax (cm μ s $^{-1}$)	Pmax (GPa)
Cu/Cu	2	0.30	30
L-J/L-J	2	0.35*	10.0*
Cu/Ag	3	0.12	5
Ta/Al	3	0.30	15
Al/Al	3	0.30	15

*For the Lennard-Jones system, velocities and pressures are given in Lennard-Jones units.

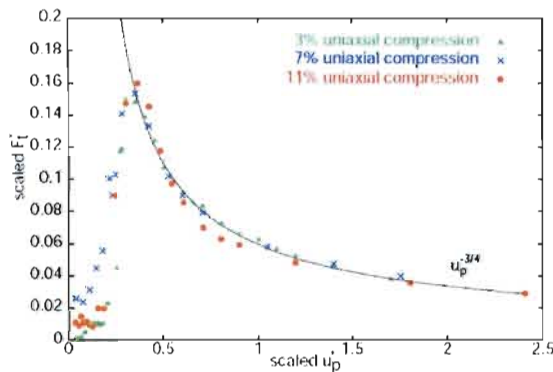
Velocity Dependence: Generic Properties of High-Velocity Sliding

There is a variety of experimental evidence that at high velocities the frictional force decreases with increasing velocity. [cf. J.E. Hammerberg and B.L. Holian, "Simulation Methods for Interfacial Friction in Solids" in Surface Modification and Mechanisms, 2004 (G.E. Totten and H. Liang, eds.) pp. 723-749]. The figure below shows simulation results for an Al(111)/Al(001) interface.

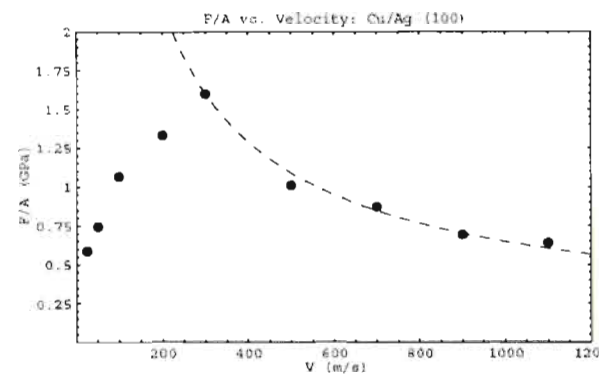
Scaled Frictional force, f/f_c , vs. Scaled Velocity, v/v_c



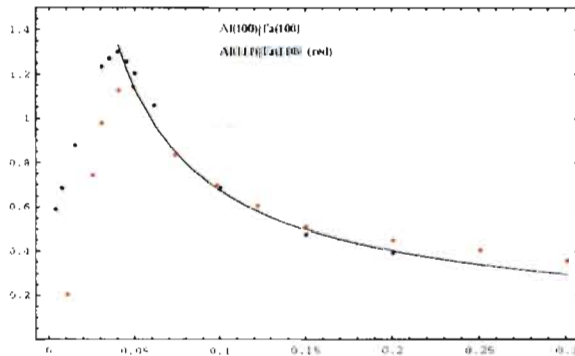
Velocity Dependence: Lennard-Jones (2D), Cu/Ag (3D), Ta/Al (3D) and Al/A (3D) Interfaces



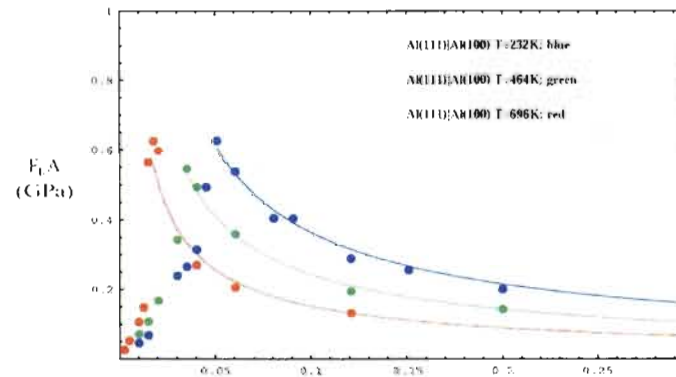
Scaled tangential force for a flat 2-D Lennard-Jones solid incommensurate interface at three compressions.
The high-velocity behavior scales as v^{-b} with $b = 3/4$.



Cu/Ag (5 GPa)



Ta/Al (15 GPa)



V_{rel} (cm/micro-sec)

Velocity Dependence: Four Regimes of Characteristic Dissipation

There are four regions in velocity that correspond to different dominant modes of dissipation.

1. $0-0.5 v_c$: anharmonic phonon dissipation
2. $0.5-1.0 v_c$: plastic deformation
3. $1.0-2.0 v_c$: structural transformation
4. $v > 2.0 v_c$: fluidization

Velocity Dependence: Anharmonic Phonon Dissipation

Low velocity regime

In this regime ($v \ll v_c$), exact results are possible and the dissipation is due to anharmonic phonons:

$$\delta F_{12} = \frac{2\pi}{\Omega^2} \sum_{\vec{q}} (\vec{q} \cdot \vec{v}) |\phi(\vec{q})|^2 \int [-S_1(\vec{q}, -\vec{q}; \omega) \text{Im} G_2^{ret}(\vec{q}, -\vec{q}; \omega + \omega_0(\vec{q})) \\ + S_2(\vec{q}, -\vec{q}; \omega) \text{Im} G_1^{ret}(\vec{q}, -\vec{q}; \omega + \omega_0(\vec{q}))] d\omega$$

where $\omega_0(\vec{q}) = \vec{q} \cdot \vec{v}$. When v approaches zero the rhs is linear in $\omega_0(\vec{q})$. $S_1(\vec{q}, -\vec{q}; \omega)$ is a dynamic structure factor defined by

$$S_1(\vec{q}, -\vec{q}; t - t') = \langle n_1(\vec{q}, t) n_1(-\vec{q}, t') \rangle_0 = \sum_{i \in \Omega_1} \sum_{j \in \Omega_1} T_F \rho_0 e^{i\vec{q} \cdot R_i(t) - i\vec{q} \cdot R_j(t')}$$

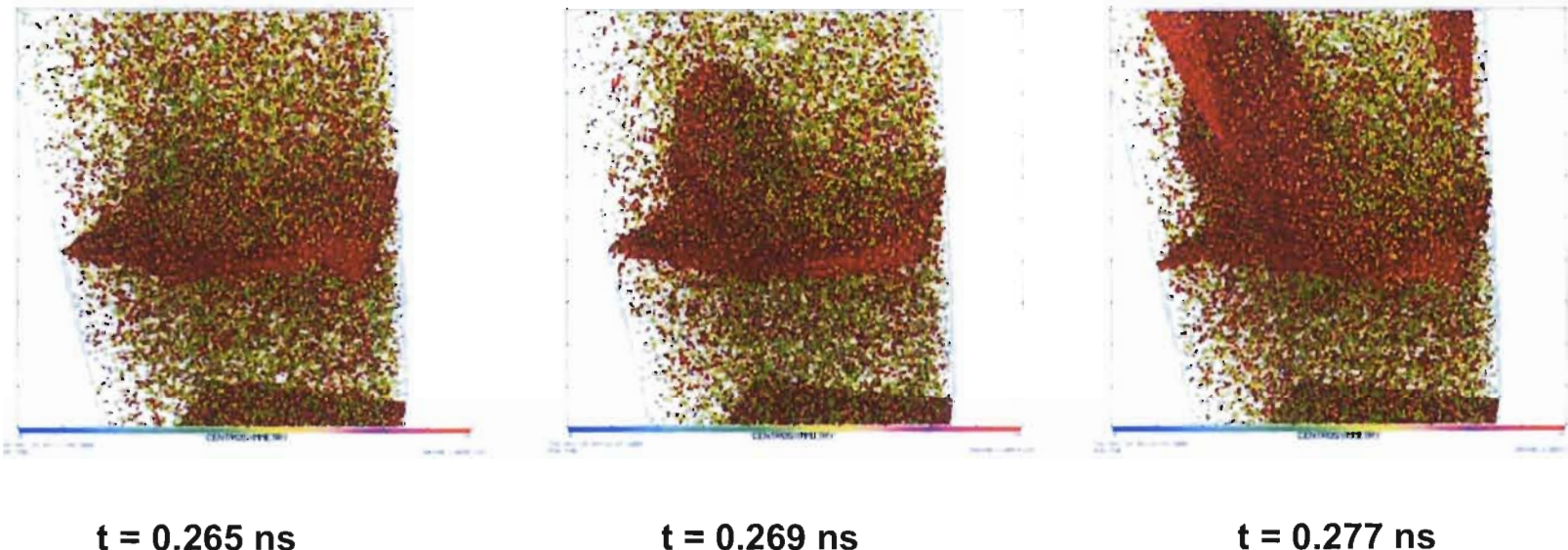
and $\text{Im} G_1^{ret}(\vec{q}, -\vec{q}; \omega + \omega_0(\vec{q}))$ is the density-density response function written as the imaginary part of the Green's function.

For an incommensurate interface these expressions lead to a linear velocity dependence at low velocities proportional to inverse phonon lifetimes from evaluation of the imaginary part of the retarded phonon Green's function.

Velocity Dependence: Plastic Deformation

Intermediate Regime ($0.5 v_c \leq v \leq v_c$): Plasticity

Al/Al stacking fault formation at $v_{rel} = 150$ m/s, $T_{res} = 696$ K



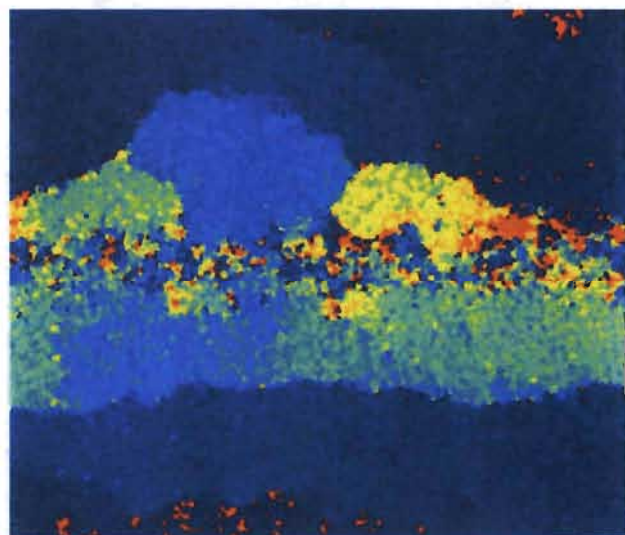
$t = 0.265$ ns

$t = 0.269$ ns

$t = 0.277$ ns

Velocity Dependence: Structural Transformation

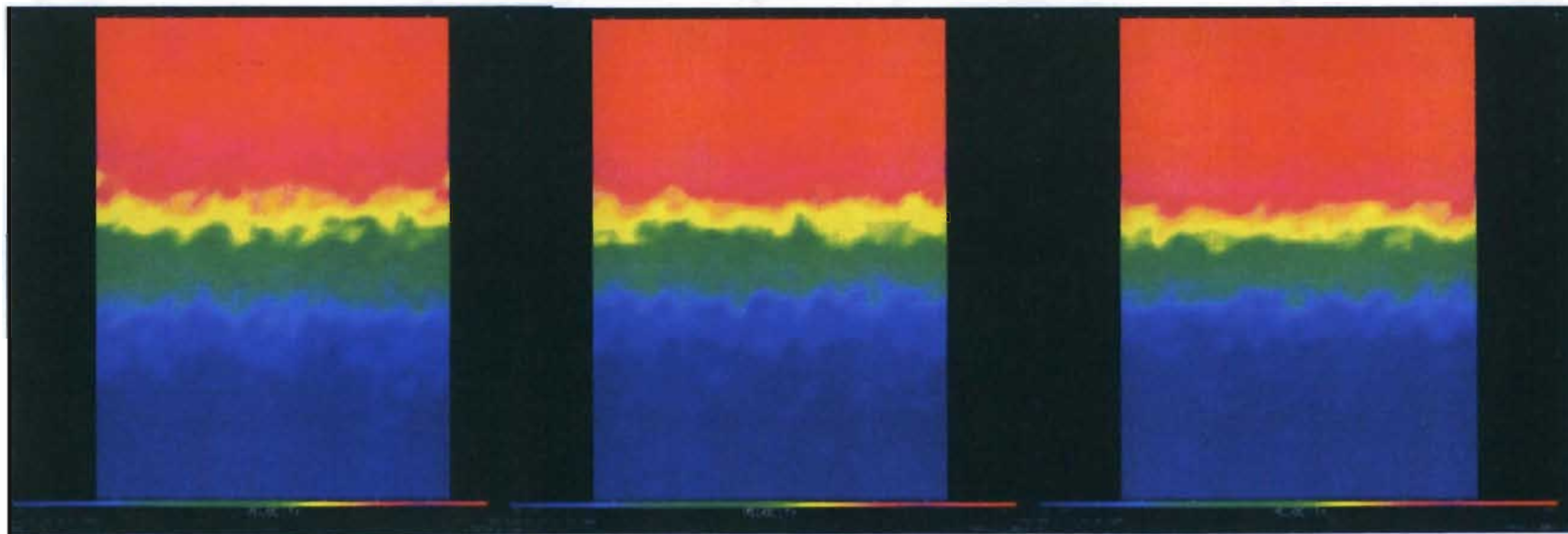
Cu (2D) $P = 30$ Gpa. $V = 0.12c_t$ Mechanical Mixing



Velocity Dependence: Structural Transformation – Fluidization

A/(111)/Al(001) interface at very high velocities exhibits confined non-laminar Couette fluid flow behavior.

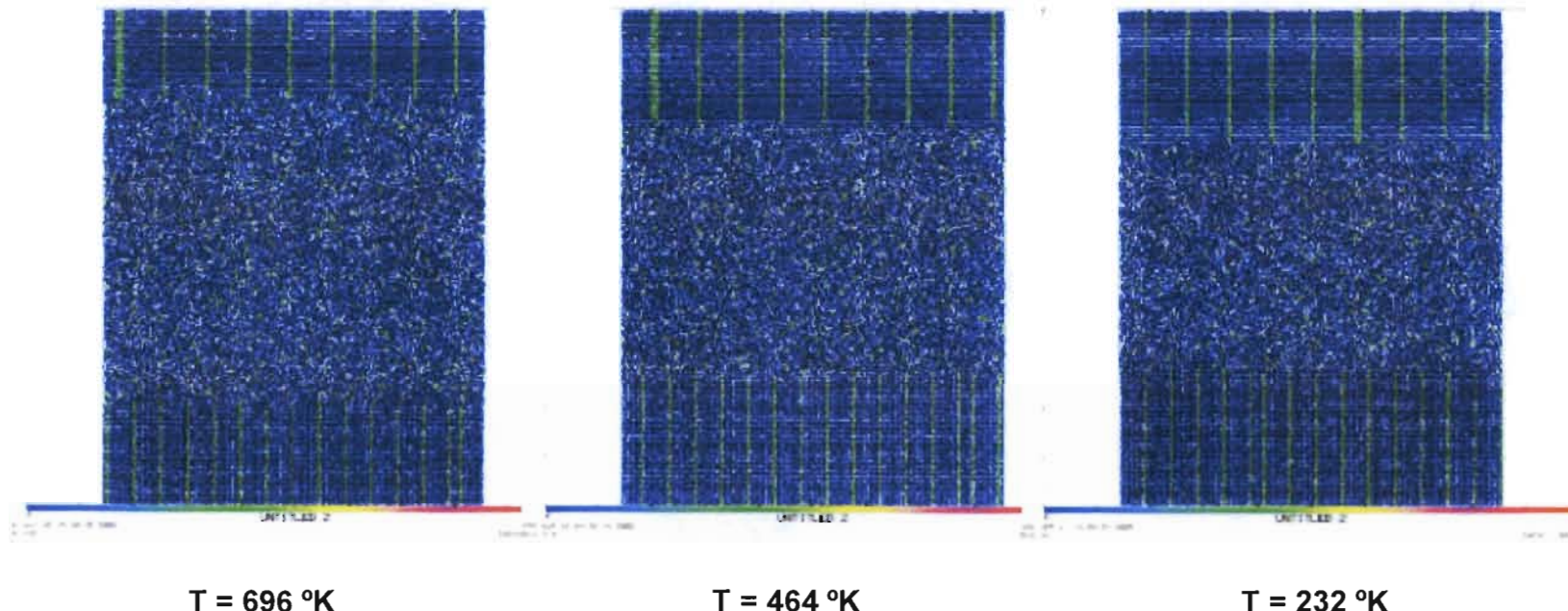
Tangential Velocity Field ($v_x(x,y)$)
 $V_{rel} = 2 \text{ km/s}$, $T_{res} = 696, 464, 232 \text{ K}^\circ$



Velocity Dependence: Structural Transformation – Fluidization

Al(111)/Al(001) interface at very high velocities and particle positions:
Couette region size depends on boundary temperature.

$V_{\text{rel}} = 2.0 \text{ km/s}$, $T_{\text{res}} = 696, 464, 232 \text{ K}^\circ$

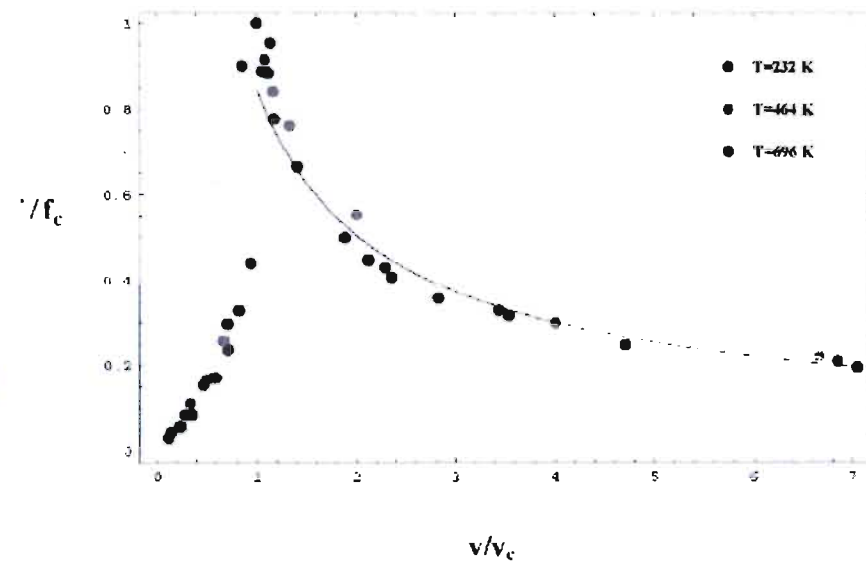
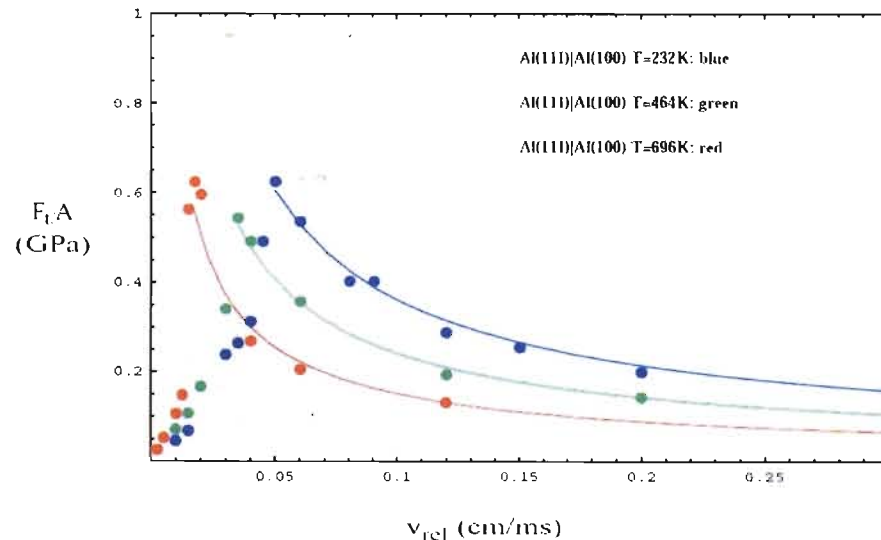


NEMD Simulations - Summary

- NEMD simulations have shown velocity weakening at high velocities for a variety of metal/metal interfaces.
- There are four regimes of deformation as velocity increases: anharmonic phonon dominated, dislocation and defect dominated, structural transformation, and fluidization.
- Material mixing occurs at the higher velocities.
- The above are qualitatively similar to the experimental picture described above.
- The velocity dependence at high velocities is well represented by a power law velocity dependence for the frictional force.

Generic Properties of the Velocity Dependence of the Frictional Force and Analysis

Al(111)/Al(001) results have shown scaling behavior:



$$P = 15 \text{ Gpa}, N_{\text{atoms}} = 1.5 \cdot 10^6$$

The Simulation Results Are Well Represented by a Scaled Function for the Tangential Force Per Unit Area.

$$f \equiv \frac{F}{A} = f_c \left(\frac{v}{v_c} \right)^{-\beta}$$

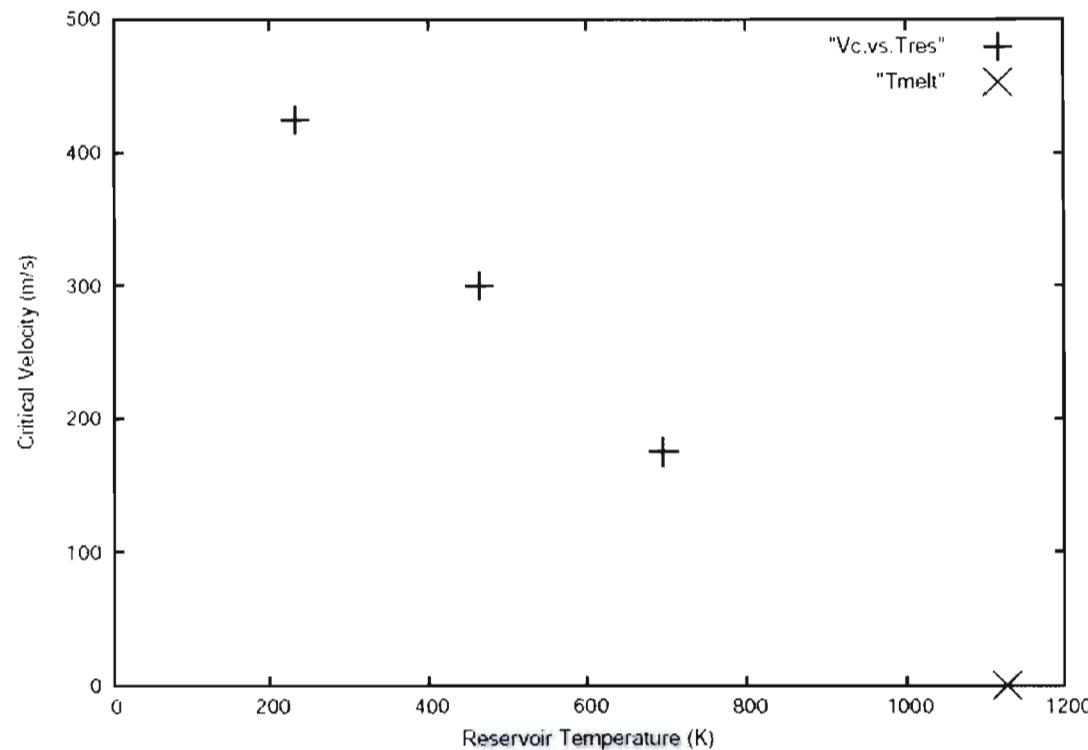
$$v_c = \frac{4 \bar{\kappa} T^*}{f_c L} \left(1 - \frac{T_0}{T^*} \right)$$

- T^* is a critical temperature at v_c and $\bar{\kappa}$ is an average thermal conductivity. $T^* = T_{\text{melt}}$ and T_0 is the boundary temperature.

$$\bar{\kappa} = \frac{1}{(T^* - T_0)} \int_{T_0}^{T^*} \kappa(T) dT$$

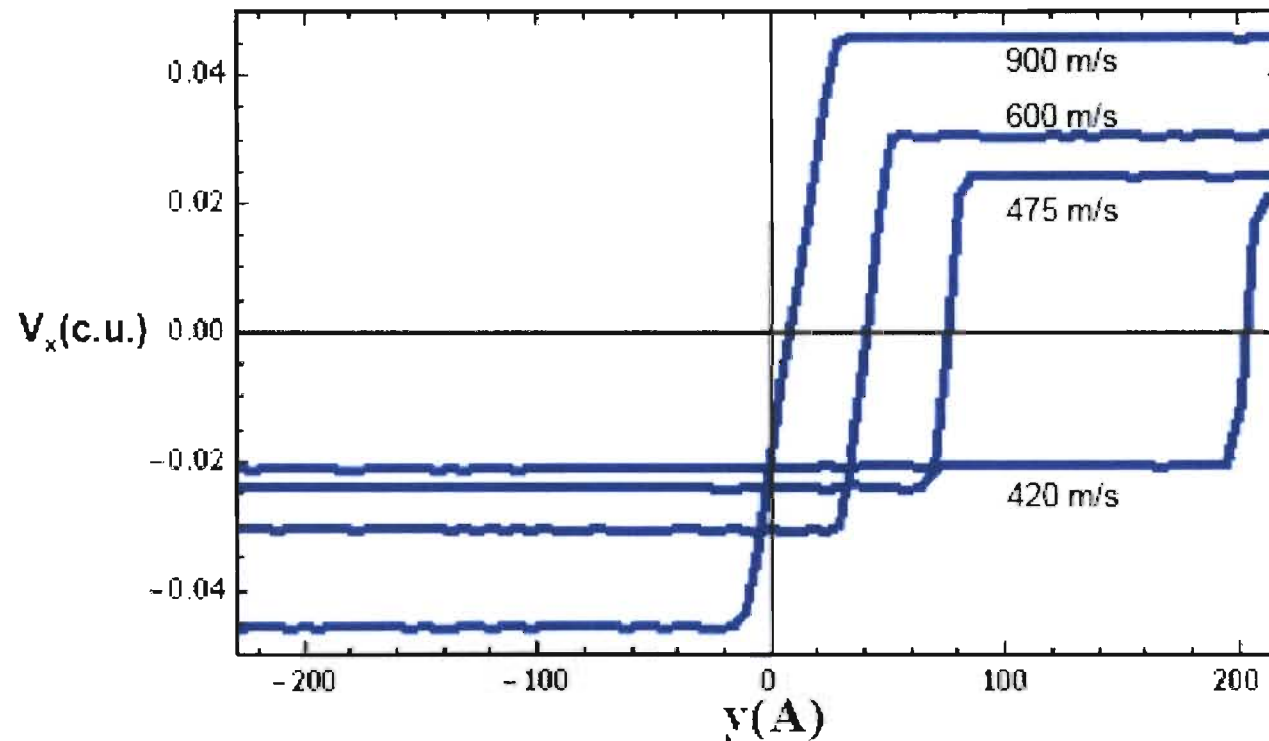
Scaling of the Frictional Force – Al/Al (cont.)

The temperature dependence of v_c is very nearly linear with respect to reservoir temperature.

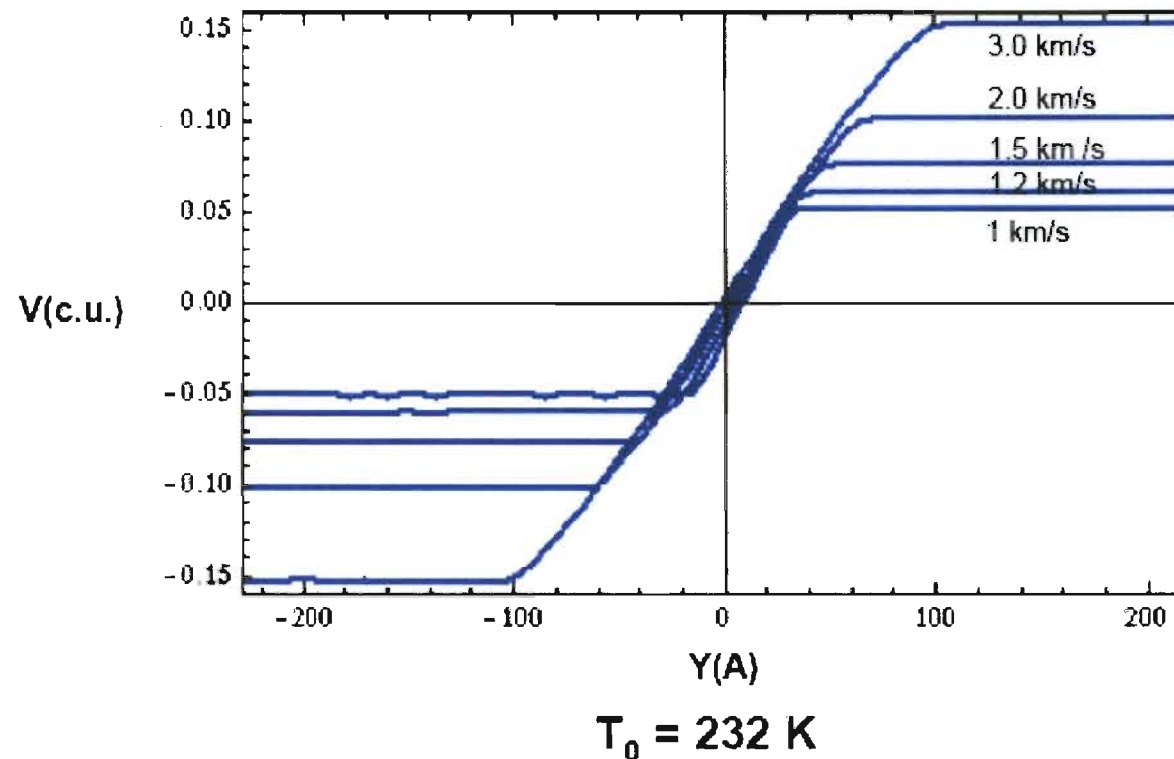


Structural Transformation for $v_c < v < v_{c1}$

- For velocities $v_c < v < v_{c1}$, a transformation front coincident with the sliding surface forms, transforming (111) material into (001) material.

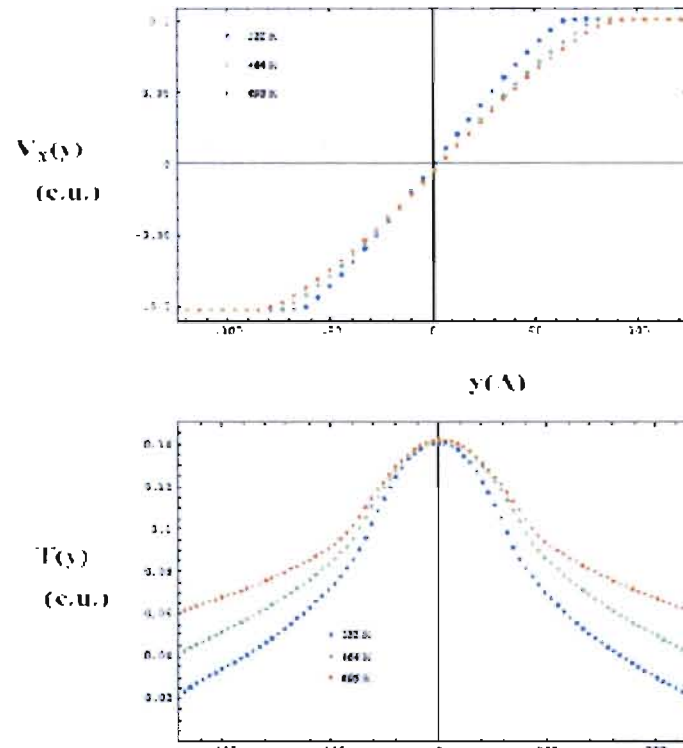


For Velocities above v_{c1} a Couette Flow Pattern Forms Characterized by a Critical Strain Rate.



The Critical Strain Rate Depends on the Boundary Temperature, and the Temperature Profile Is Parabolic in the Fluid Region.

Velocity and Temperature Profiles: $v_{\text{rel}}=2 \text{ km/s}$, $T_{\text{res}}=232, 464, 696 \text{ }^{\circ}\text{K}$
(1 c.u. $T = 11605 \text{ }^{\circ}\text{K}$, 1 c.u. $V = 9.823 \text{ km/s}$)



The Velocity Dependence of the Interface Temperature in the High-Velocity Regime May Be Analyzed in Terms of Fluid and Mechanical Quantities.

$$T(0) = T_m + \frac{1}{8} \left(\frac{\kappa}{\eta} \right)^{-1} v^2$$

$$T(0) = T_m + \frac{1}{8} \left(\frac{c_v}{Pr} \right)^{-1} v^2$$

$$T(0) = T_m + \frac{1}{8} \left[\frac{f}{(\kappa) \dot{\epsilon}_c} \right] v^2$$

$$T(y) = T(0) - \frac{1}{2} \left(\frac{\kappa}{\eta} \right)^{-1} \dot{\epsilon}_c^2 y^2$$

where $\dot{\epsilon}_c$ is the critical strain rate in the Couette regime, κ is the thermal conductivity, η is the fluid viscosity, c_v is the specific heat and Pr is the Prandtl number, and the brackets denote thermal averages between $T(0)$ and T_m and between $T(0)$ and $T(y)$ in the last equation.

These Relations and the Scaled Form for F Imply Relationships for T(0) and the Critical Strain Rate.

$$T(0) = T_m + \frac{1}{8} \left[\frac{f_c v_c^\beta}{\langle \kappa \rangle \dot{\epsilon}_c} \right] v^{1+\alpha} \quad (\alpha = 1 - \beta)$$

$$\dot{\epsilon}_c = A \frac{f_c}{\langle \kappa \rangle} v_c^\beta$$

where the second expression assumes the result from the NEMD simulations which show the values for T(0) independent of v_c in the Couette regime.

There is also a relationship between v_c and v_{c1} :

$$\frac{v_{c1}}{v_c} = \left(\frac{\eta(T_m) \dot{\epsilon}_c}{f_c} \right)^{-\frac{1}{\beta}}$$

Summary

- The tangential force between ductile metals exhibits a generic velocity dependence.
- There is a critical velocity, v_c , beyond which the tangential force decreases and the dominant dissipative mechanism changes from plastic deformation to structural transformation and fluidization at the highest velocities.
- There is a second critical velocity, $v_{c1} > v_c$, beyond which the fluid interface exhibits Couette flow. In this regime the tangential force is determined by a critical strain rate, the fluid viscosity and thermal conductivity.
- The tangential force for $v > v_c$ exhibits scaling behavior with a power law exponent, $\beta = 3/4$, and $f \sim (v/v_c)^{-\beta}$.
- For $v > v_{c1}$, the flow is non-laminar and mixing.

Summary

- Ultimately, one would like to have a constitutive model for the tangential force to be used in macroscopic engineering simulation computer models:

$$\frac{F_t}{A} = f(P, T; \epsilon_p, v_{rel})$$

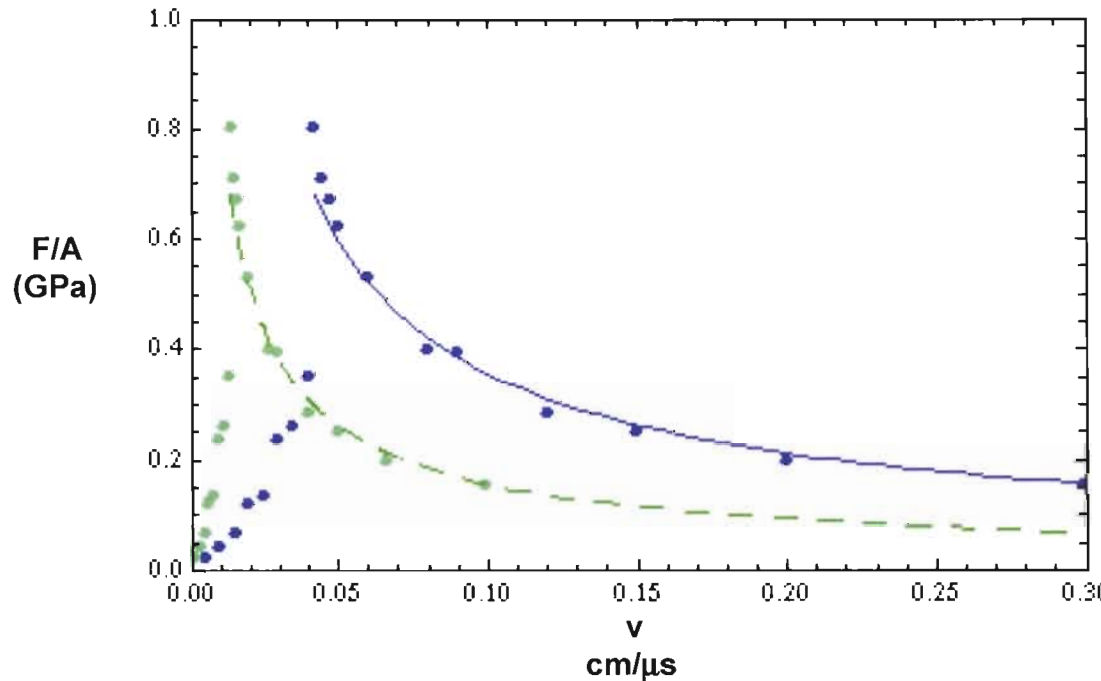
where A is surface area, P pressure, T temperature, ϵ_p plastic strain, and v_{rel} the relative velocity. The above expressions are the basis for such a model.

Al Perfect Crystal Scaling

- To investigate length scaling we have taken a large (7.5 M) atom sample with a normal dimension of 154 nm.
- The sample consisted of two (110) faces rotated 90 degrees to form an incommensurate interface.
→
- This represents $L \sqrt{3}L$
- Reservoir temperature: 300 °K
- Pressure 15 Gpa
- Sliding direction along $\langle 100 \rangle$
- System size 7.4844 M atoms with sample dimensions (27.092, 153.773, 27.092) nm

System size scaling

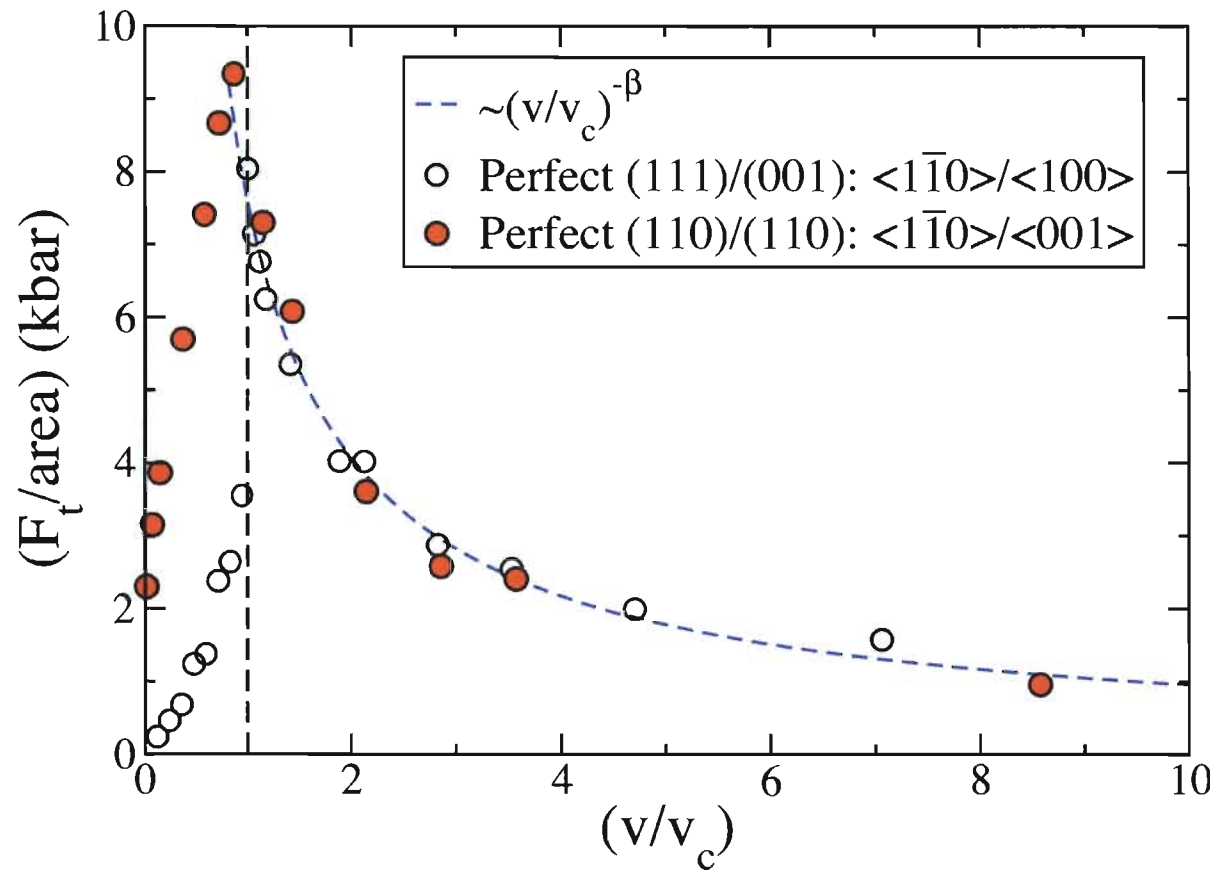
The critical velocity is given by $v_c = 4 \frac{\bar{K}T^*}{f_c L} \left(1 - \frac{T}{T^*}\right)$



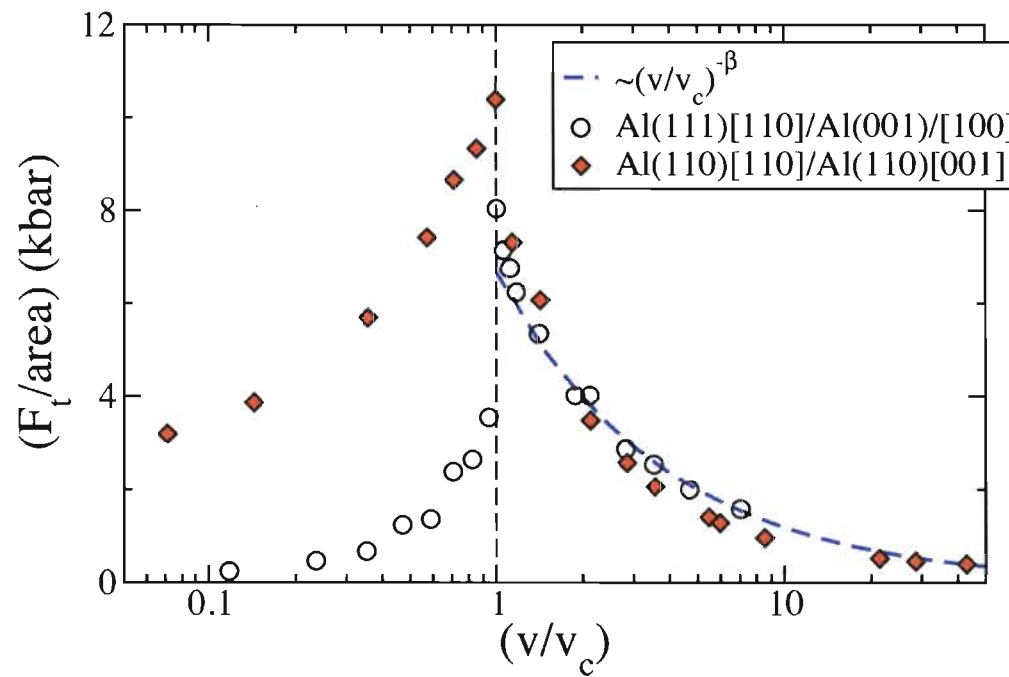
Blue curve: (111)/(001) single crystal sliding

Green curve: same data scaled to 3xL assuming no change in f_c

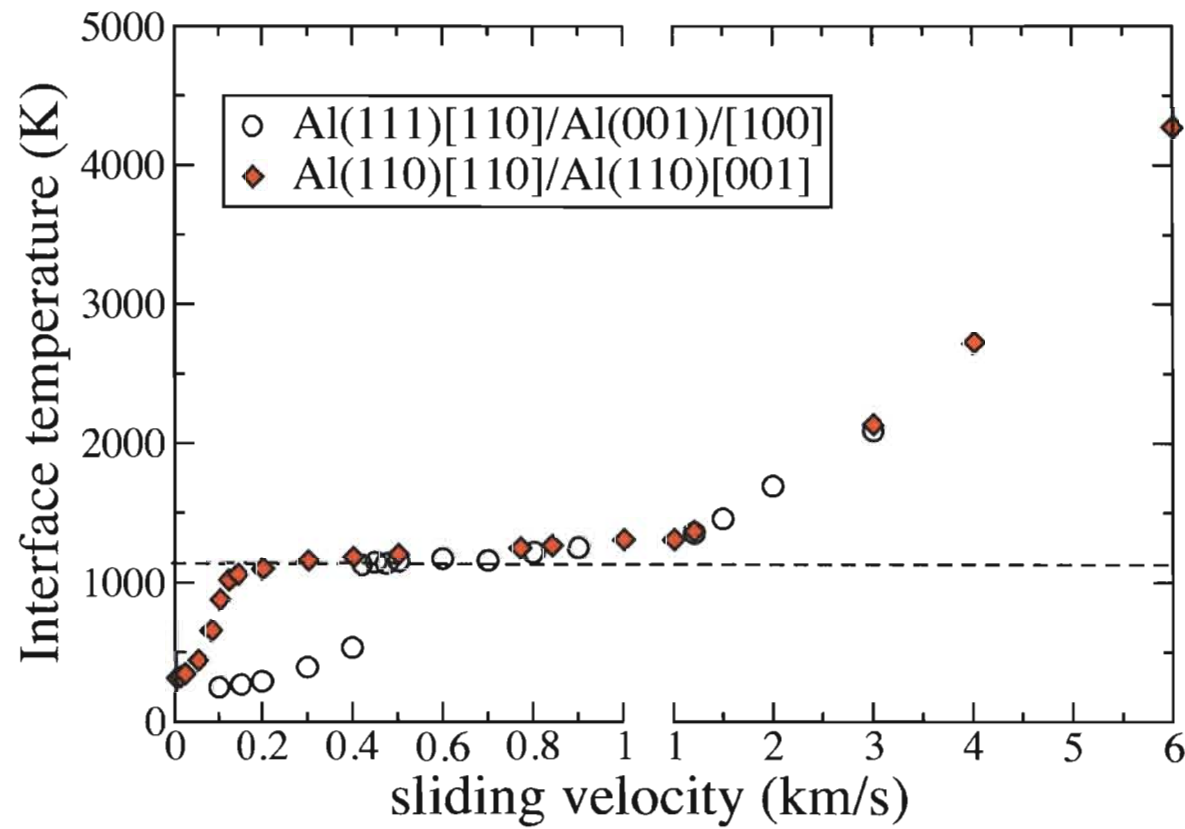
Size Scaling - Tangential Force



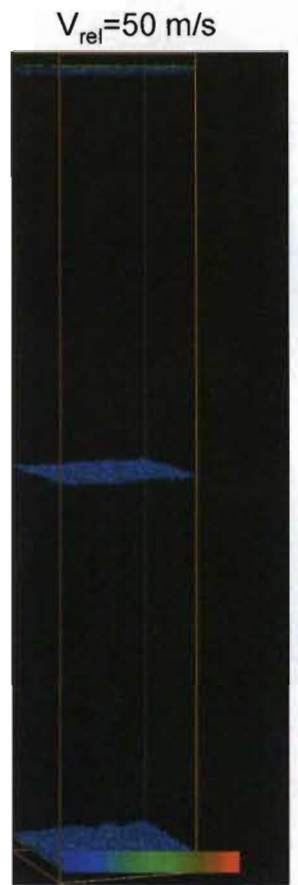
Size Scaling - Tangential Force



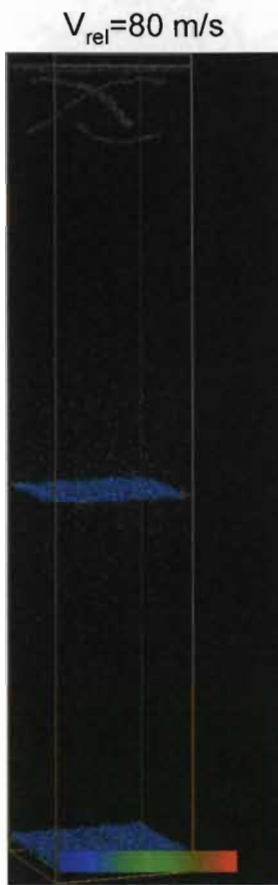
Scale Independence of Interface Temperature in the Couette Regime



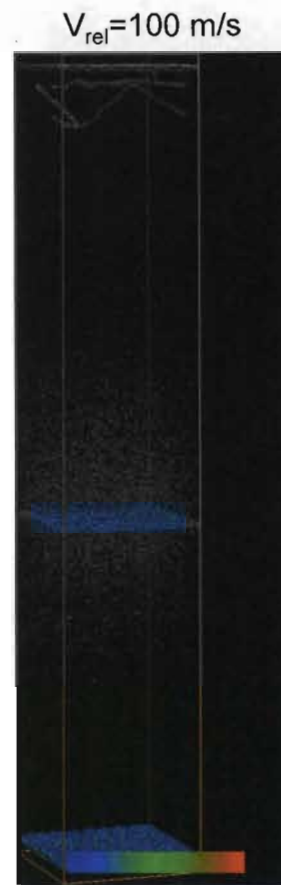
Normal Interface Motion Al (110)/(110): $\langle 1\bar{1}0 \rangle/\langle 001 \rangle$ Centro-Symmetry Parameter



$T_{\text{int}} = 440 \text{ °K}$
 $V_{\text{front}} = 0 \text{ m/s}$



$T_{\text{int}} = 654 \text{ °K}$
 $V_{\text{front}} = 3 \text{ m/s}$



$T_{\text{int}} = 875 \text{ °K}$
 $V_{\text{front}} = 5.6 \text{ m/s}$

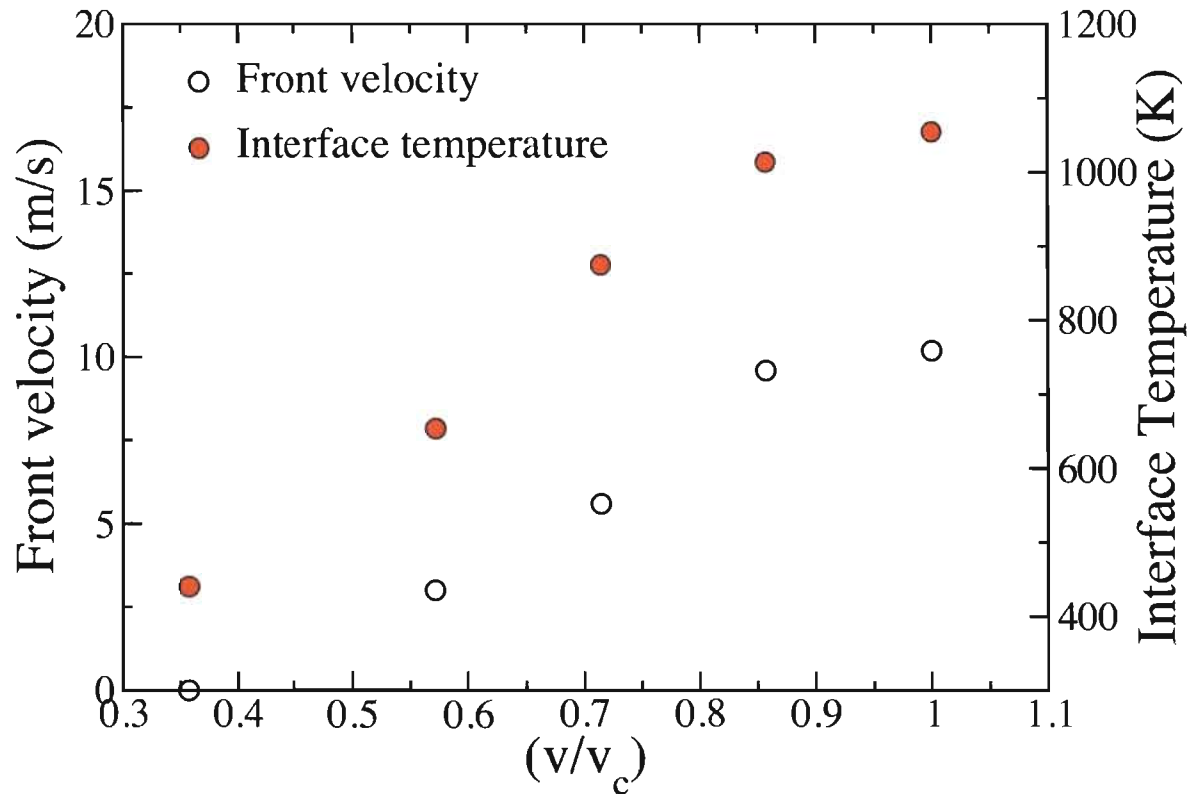


$T_{\text{int}} = 1015 \text{ °K}$
 $V_{\text{front}} = 9.6 \text{ m/s}$

($t = 2 \text{ ns}$)

Normal Interface Motion Al (110) / (110) : $\langle 1\bar{1}0 \rangle / \langle 001 \rangle$

Interface velocity and temperature



Summary

- We have studied the sliding behavior for a 7.5 M Al(110)/Al(110) perfect crystal at 15 GPa as a function of relative sliding velocity.
- The general features are qualitatively similar to smaller scale (1.4 M) atom simulations for Al(111)/Al(110) single crystal sliding.
- The critical velocity, v_c , agrees with the size scaled v_c .
- For velocities below v_c , the tangential force for this orientation (110)/(110) exceeds that for the scaled (111)/(001) orientation.

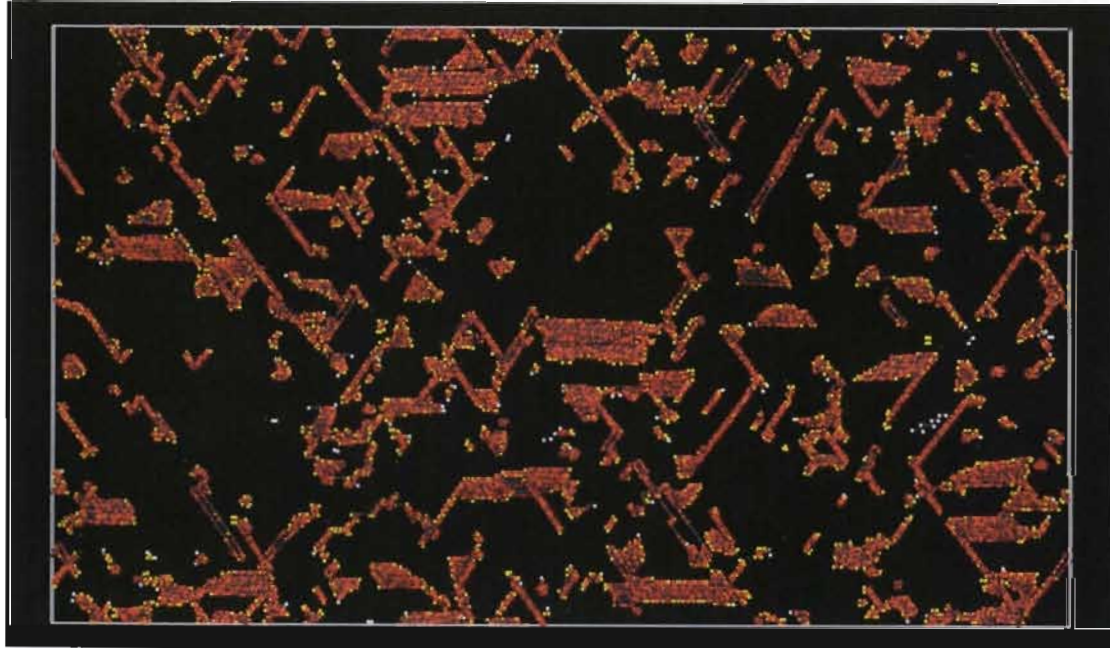
Summary (cont.)

- The range for a transformation front normal to the interface extends from 80 m/s – 800 m/s .
- The interfacial temperature in the moving interface regime for the (110)/(110) orientation is ~550 K at the lowest velocities, rising to 1100 K at v_c ($T_m = 1127$ K at 15 GPa).
- Moving interface velocities are < 12 m/s.
- The upper critical velocity, v_{c1} , is scale independent and depends only on confined fluid properties.

Al Defective Crystal

- The parameters in the previous expressions, f_c , $\bar{\kappa}$, and T^* depend on defect structure.
- To investigate this we have taken a large (19 M) atom sample with a large density of pre-existing defects to compare with the single crystal results.
- The defective sample consisted of two (110) faces rotated 90 degrees to form an incommensurate interface.
- The defective crystal contained a large density of dislocations and stacking faults.

Al Defective Crystal



Defective isotropic crystal was generated by

- quasi-isentropic compressing a defect-free Al crystal along the (110) direction to a pressure of about 20 GPa.
- followed by an isothermal expansion to a near isotropic stress state of 15 GPa.

Defect density = $2\text{-}6 \times 10^{12} \text{ cm}^{-2}$.

Al Defective Crystal Sliding (110)/(110)

- Sliding direction along $<100>$
- System size 19.152 M atoms with sample dimensions (433.12, 1482.44, 433.12)
- Previous single crystal (111)/(001) simulations were for 1.4 M atoms with system sizes of (224.03, 504.51, 189.28)
- Pressure: 15 GPa in both

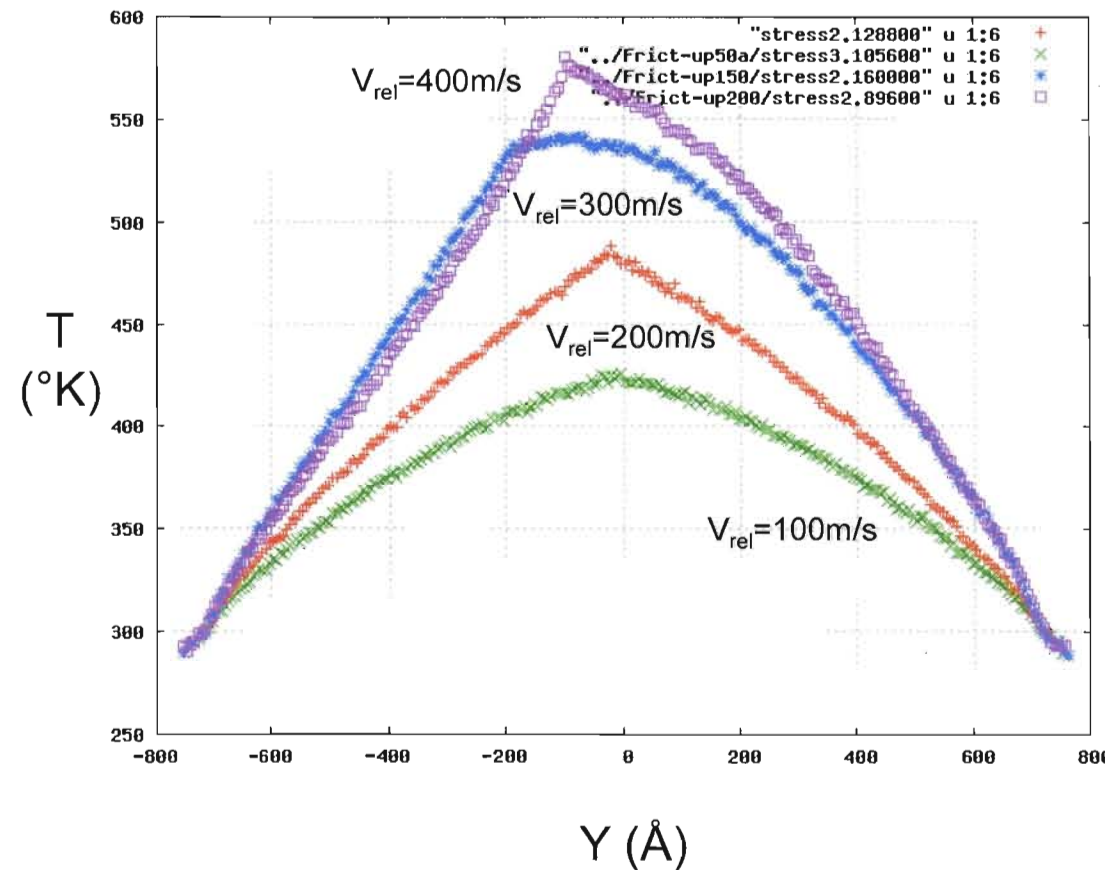
Al Defective Crystal Sliding (110)/(110)

- We present results for sliding velocities of 100, 200, 300, and 400 m/s for the defective crystal.
- We have also considered velocities of 100 and 600 m/s for a perfect crystal with the same normal dimension.
- The table summarizes the results for the defective crystal.

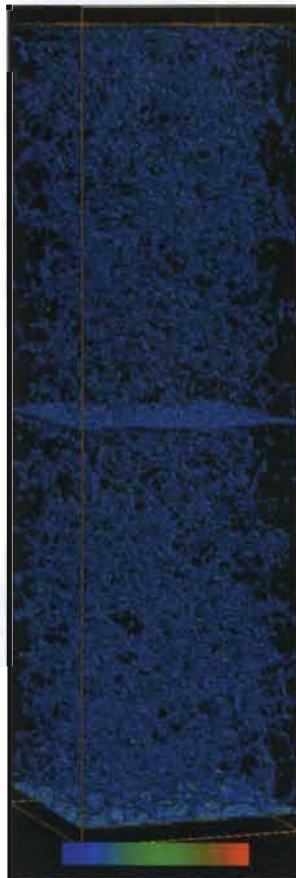
Al Defective Crystal Sliding (110)/(110) Results

Sliding Velocity (m/s)	F_{tang}/A GPa	Interface Temp °K	N_{Res}	In-plane length Ångstrom
20	0.16	385	548170	433.12
50	0.186	392	548170	433.12
100	0.29	414	548170	433.12
120	-----	445	548170	433.12

Temperature Profiles: Defective Al



Normal Interface Motion Defective Al Centro-Symmetry Parameter



$V_{\text{rel}} = 100 \text{ m/s}$



$V_{\text{rel}} = 200 \text{ m/s}$

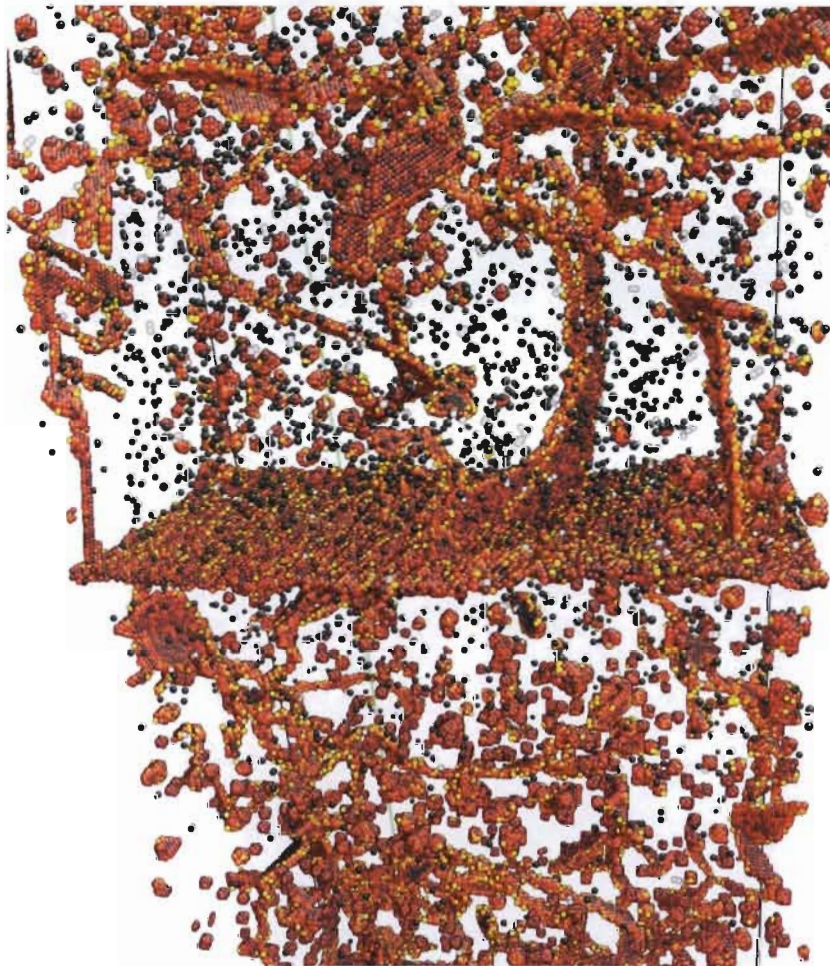


$V_{\text{rel}} = 300 \text{ m/s}$

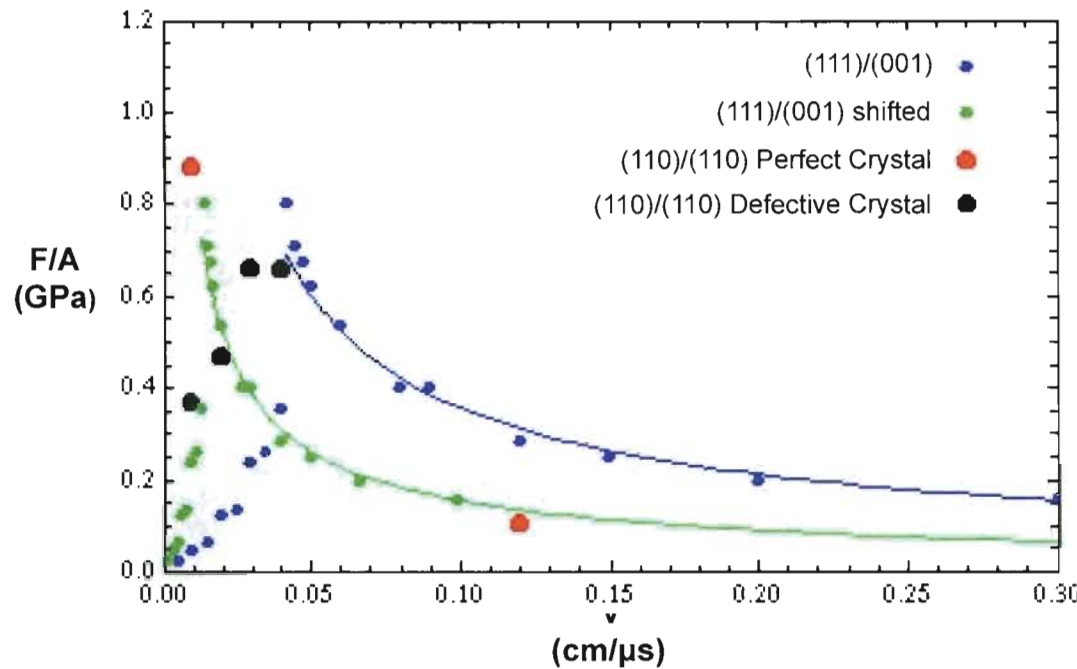


$V_{\text{rel}} = 400 \text{ m/s}$

Al Defective Crystal Centro-symmetry parameter $v_{rel}=300$ m/s , enlarged view



Results for (110)/(110) sliding



Blue curve: (111)/(001) single crystal sliding

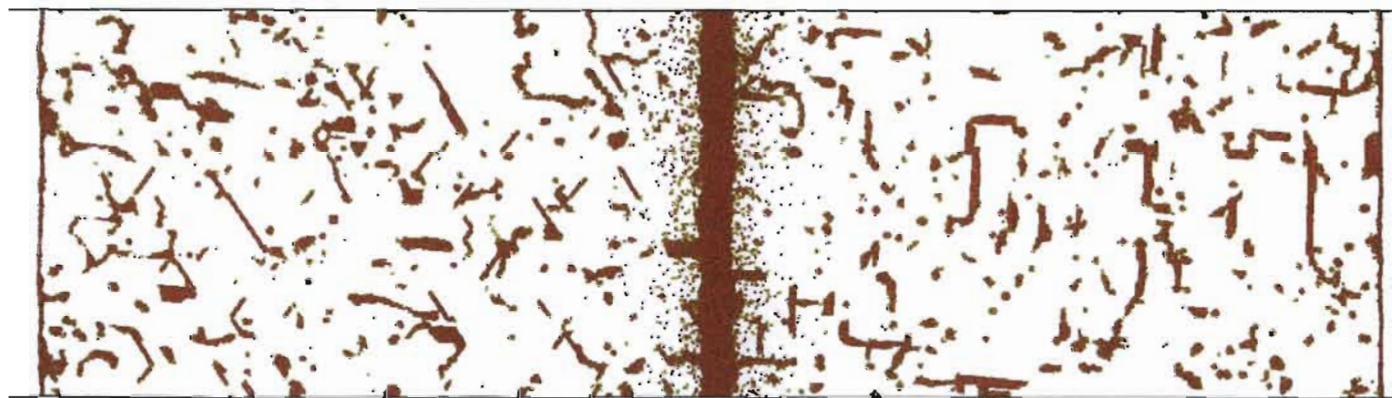
Green curve: same data scaled to 3xL assuming no change in f_c

Red points: Perfect Crystal (110)/(110) sliding

Black points: Defective Crystal (110)/(110) sliding

Preliminary results for (110)/(110) sliding

Formation of a fluid layer for $v = 420$ and 1200 m/s



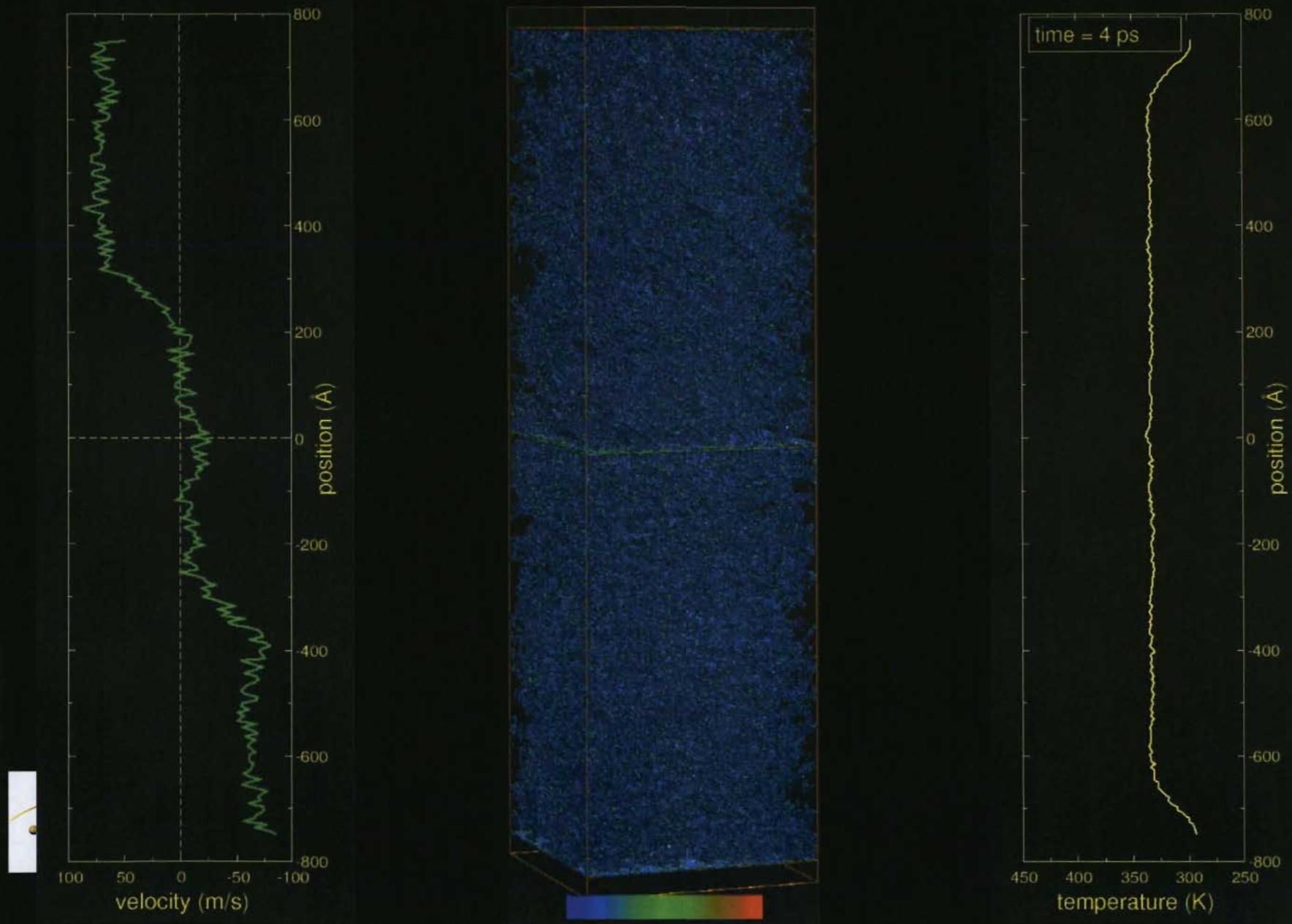
Summary

- We have studied the sliding behavior for a 19 M Al(110)/Al(110) defective crystal at 15 GPa as a function of relative sliding velocity.
- The general features are qualitatively similar to smaller scale (1.4 M) atom simulations for Al(111)/Al(110) non-defective single crystal sliding.
- The critical velocity, v_c , is larger for the defective crystal than the size scaled v_c .
- The lower velocity tangential force is depressed relative to the perfect crystal.

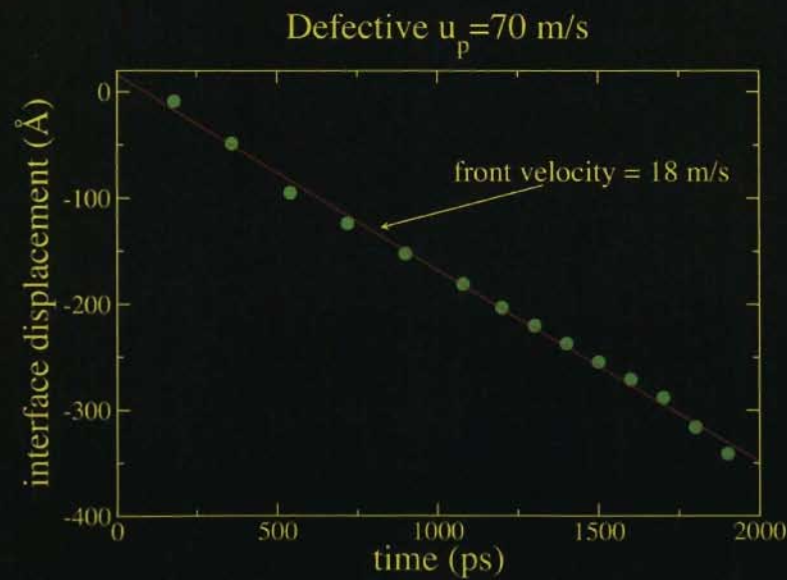
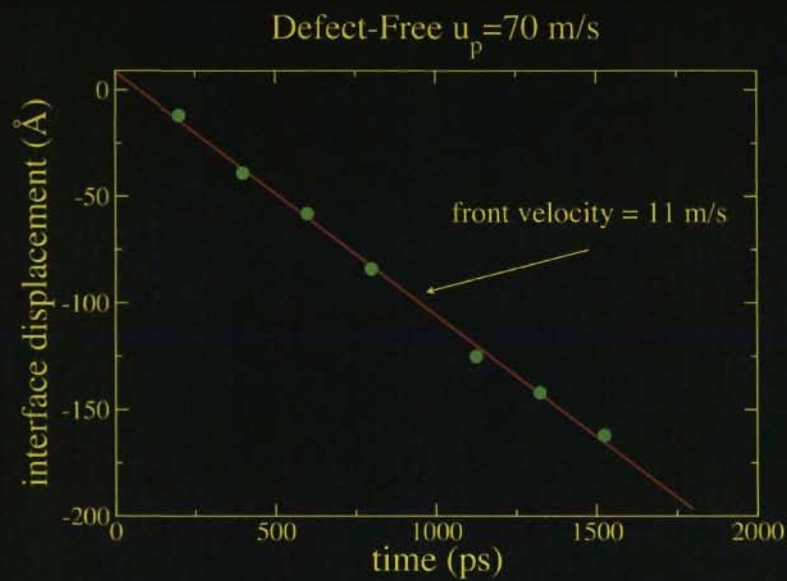
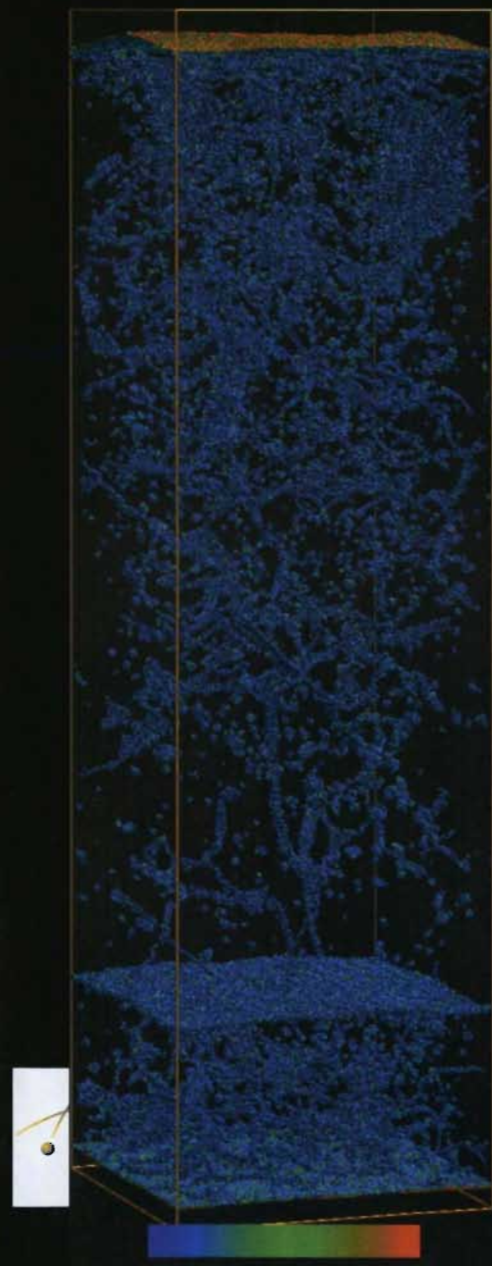
Summary (cont.)

- The critical temperature, T^* , is depressed relative to the perfect crystal.
- These conclusions are consistent with a lower value for f_c for the defective crystal.
- The detailed features of structural transformation and the high velocity regime remain to be mapped.

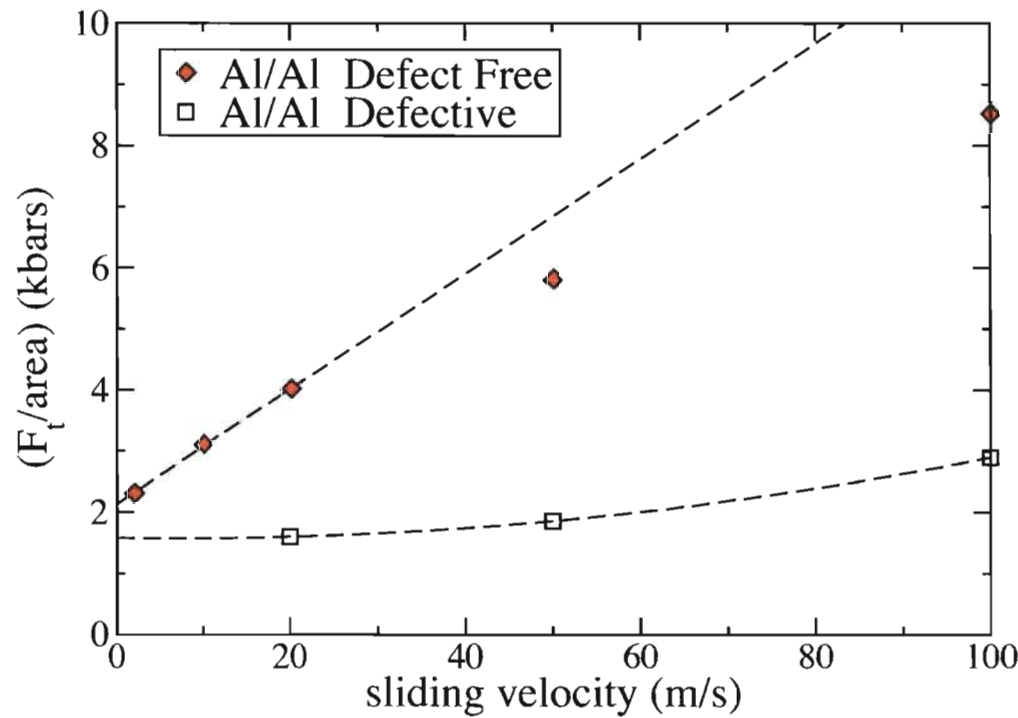
Al-Al Defective crystal $u_p=70$ m/s



Interface velocity



Lower velocity dependence of the frictional force for defective and defect free Al-Al interfaces



Polycrystalline Aluminum

Polycrystalline Aluminum samples were created via a process of Voronoi construction followed by annealing.

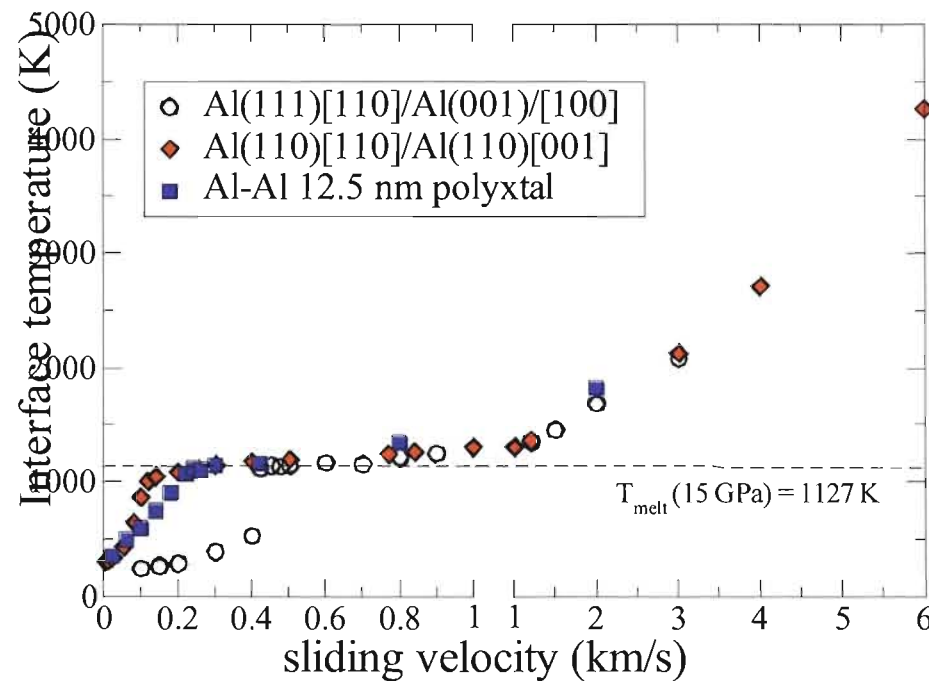
The resulting sample with grain size 12.5 nm had dimensions (385.0, 770.0, 385.0) nm. 19 nm grain sizes have also been considered.

The upper workpiece was formed by translating the lower workpiece and Rotating it by 90 degrees about the y-axis.

The nominal pressure was 15 Gpa and for these simulations the volume was fixed. The boundary reservoir temperature was 300K.

Polycrystalline Aluminum

Interface temperature vs. relative velocity

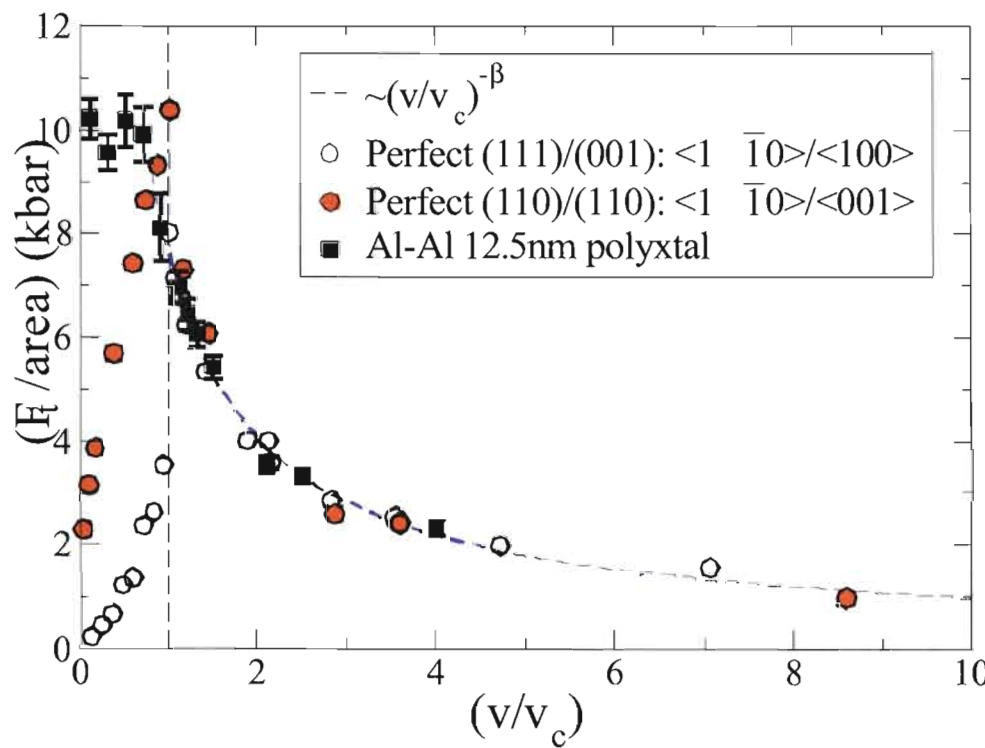


The critical velocity determined from the temperature profile is

$$v_c \approx 180 - 200 \text{ m/s}$$

Polycrystalline Aluminum

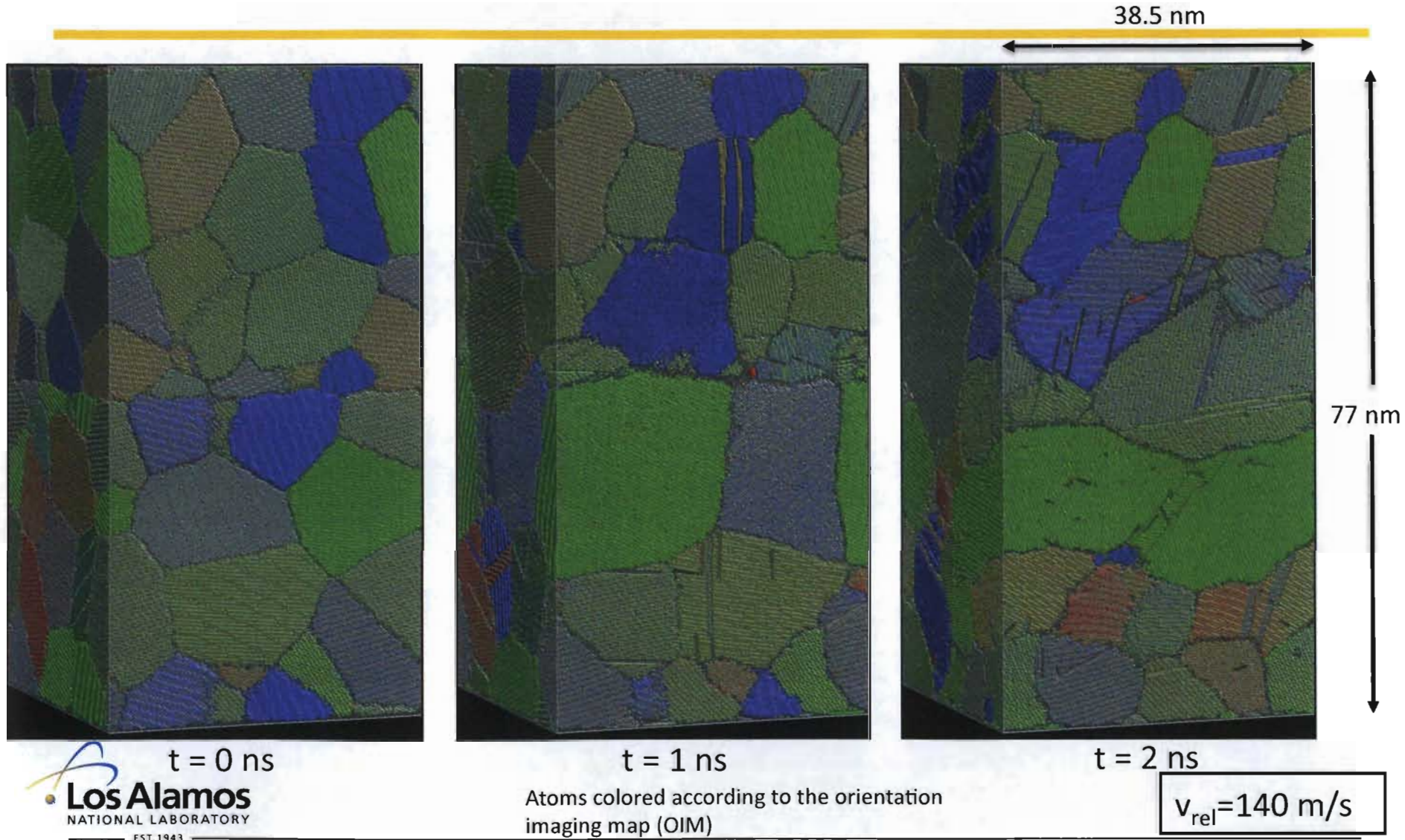
Tangential force per unit area vs. scaled relative velocity



The critical force per unit area determined from the power law: ~ 10 kbar

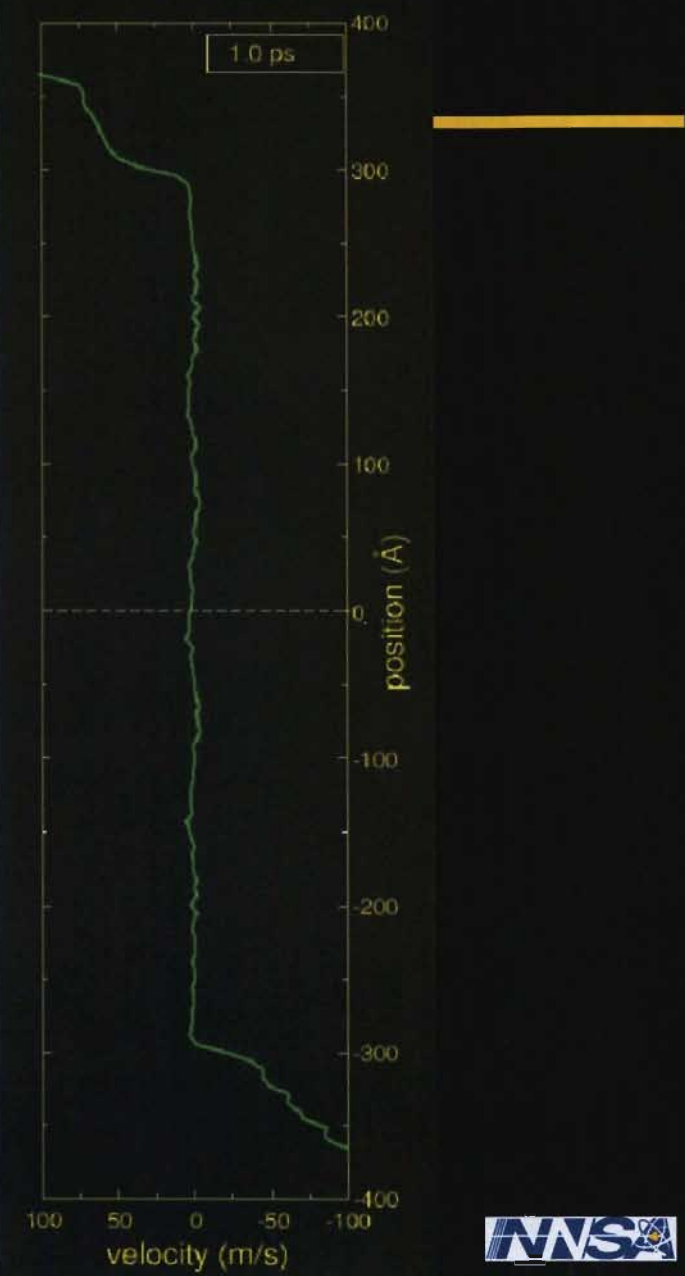
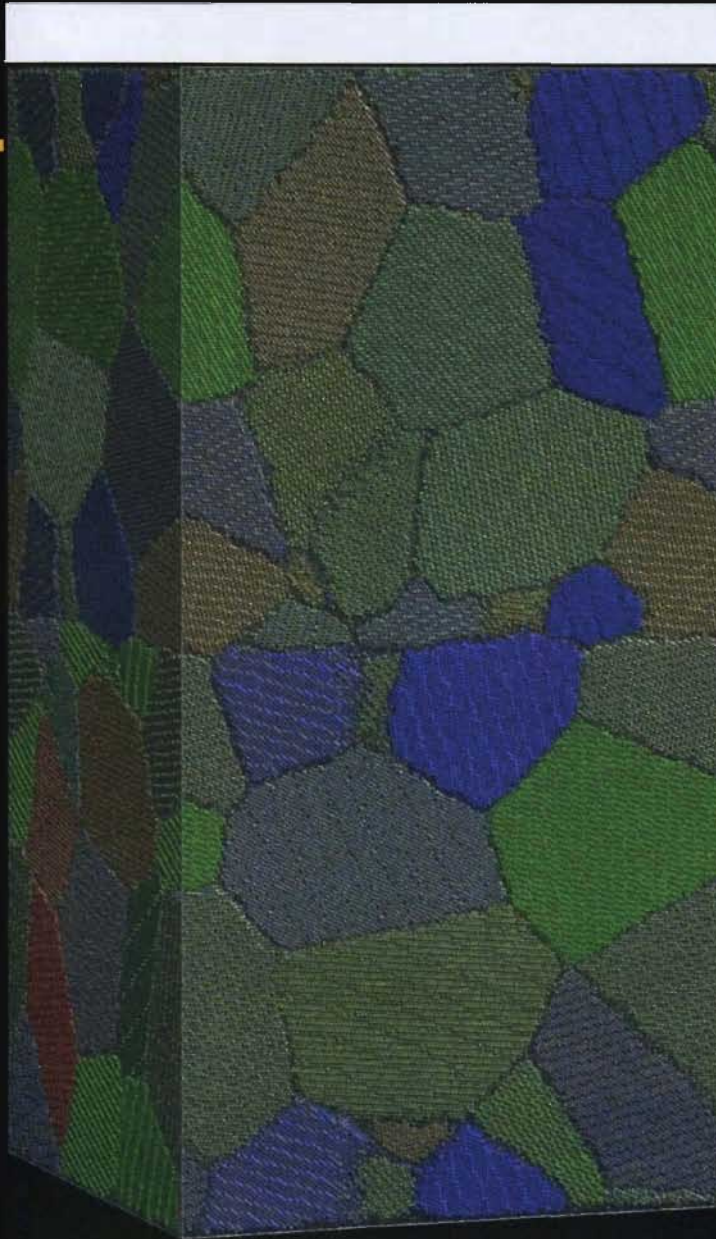
Polycrystalline Aluminum: averaged grain size = 12.5 nm

The initial grain structure at the sliding interface coarsens, resulting in highly elongated grains at velocities $< v_c = 200$ m/s



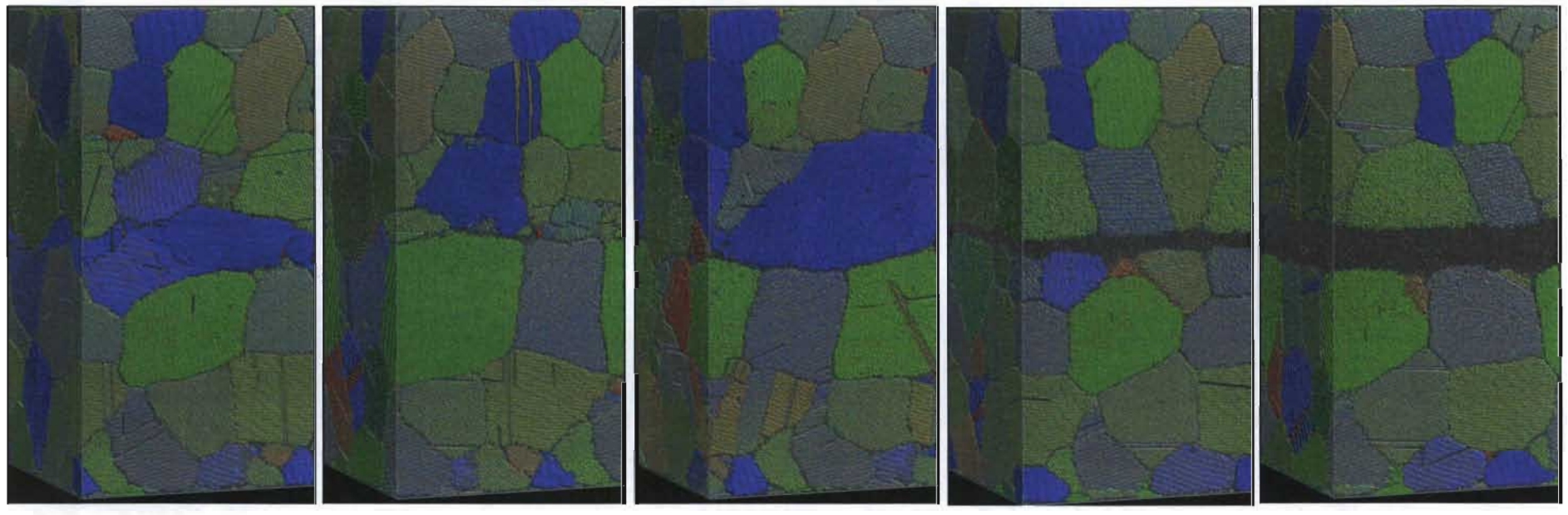
Polycrystalline Aluminum: averaged grain size = 12.5 nm

$v_{\text{rel}} = 180 \text{ m/s}$



Polycrystalline Aluminum

The initial grain structure at the sliding interface coarsens, resulting in highly elongated grains at velocities $< v_c = 200$ m/s



$v_{\text{rel}} = 60$ m/s

$v_{\text{rel}} = 140$ m/s

$V_{\text{rel}} = 180$ m/s

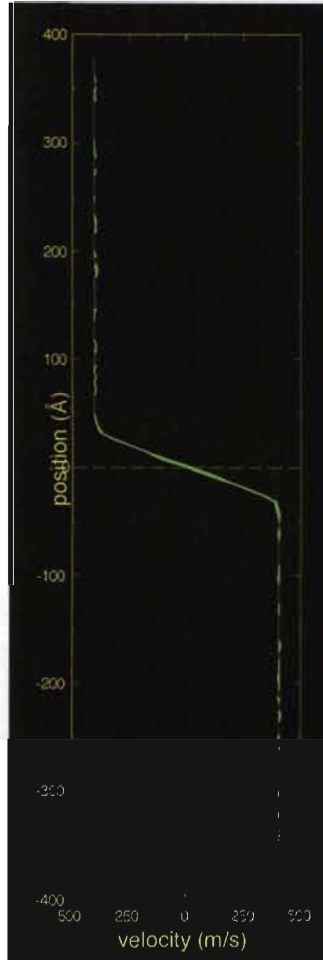
$v_{\text{rel}} = 420$ m/s

$v_{\text{rel}} = 800$ m/s

$t = 1$ ns

Polycrystalline Aluminum

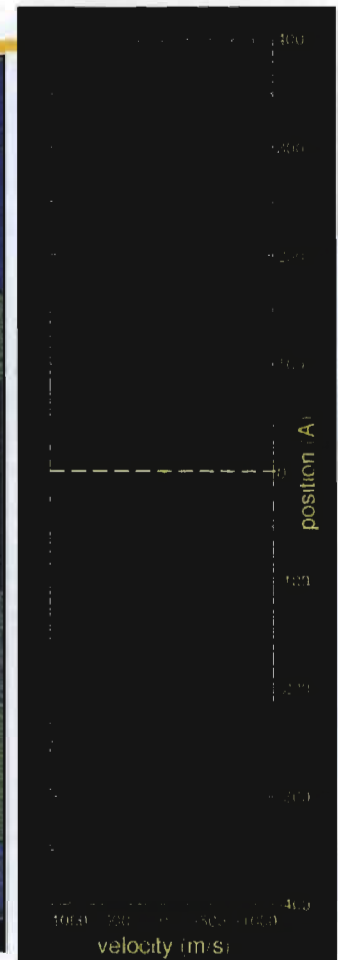
For $v > v_{c1}$ a Couette flow pattern develops



$v_{\text{rel}} = 800 \text{ m/s}$



$v_{\text{rel}} = 2000 \text{ m/s}$



Conclusions

- The results of NEMD simulations for Al interfaces have shown the applicability of a scaling interpretation for high velocity sliding.
- For velocities greater than an upper critical velocity a Couette fluid layer develops with a power law behavior in the velocity dependence of the tangential force.
- For velocities near and above a lower critical velocity structural transformation occurs with interface temperatures near the melting temperature.
- Recent results for polycrystalline Al samples with grain sizes of 12.5 nm and 19 nm indicate, for velocities below the lower critical velocity, very large plasticity and deformation induced grain coarsening with enhanced frictional force relative to single crystal results.